

**DETERMINATION OF REACTIVITY RATIOS FOR
ACRYLONITRILE/METHYL ACRYLATE RADICAL
COPOLYMERIZATION VIA NONLINEAR METHODOLOGIES
USING REAL TIME FTIR**

by

Kenton B. Wiles

Thesis Submitted to the Faculty of the
Virginia Polytechnic Institute and State University
in partial fulfillment of the requirements for the degree of

Master of Science
in
Chemistry

APPROVED:

Dr. James E. McGrath, Chairman

Dr. Judy S. Riffle

Dr. Allan R. Shultz

August 7, 2002
Blacksburg, Virginia

Keywords: Reactivity Ratios, Acrylonitrile, Methyl Acrylate, AIBN, DMF,
In situ FTIR, Nonlinear Analysis.

Copyright 2002, Kenton B. Wiles

**DETERMINATION OF REACTIVITY RATIOS FOR
ACRYLONITRILE/METHYL ACRYLATE RADICAL COPOLYMERIZATION
VIA NONLINEAR METHODOLOGIES USING REAL TIME FTIR**

Kenton B. Wiles

J. E. McGrath, Chairman

Chemistry

(ABSTRACT)

Reactivity ratios for the homogeneous free radical initiated copolymerization of acrylonitrile and methyl acrylate were measured by NMR on isolated, low conversion copolymers and by real time *in situ* FTIR. The system utilized azobisisobutyronitrile (AIBN) initiator in dimethyl formamide (DMF) at 62°C. The FTIR technique allowed rapid generation of extensive copolymer compositions, which permitted application of nonlinear least squares methodology for the first time to this copolymer system. Thus, reactivity ratios at the 95% confidence level were determined to be 1.29 ± 0.2 and 0.96 ± 0.2 for acrylonitrile and methyl acrylate, respectively. The results are useful for the development of acrylonitrile (<90%) melt processable copolymer fibers and films, which could include precursors for carbon fibers.

Acknowledgements

The author would like to express his gratitude to Dr. J. E. McGrath for his support and guidance throughout this research project.

The author would also like to extend his thanks to the rest of his advisory committee, Dr. J. S. Riffle and Dr. A. R. Shultz, for their helpful suggestions and insight.

Finally, he would like to express a special thanks to his wife, Natasha, and his parents Mr. and Mrs. Don and Jeanette Wiles for their moral support.

Table of Contents

Chapter I. INTRODUCTION	1
Chapter II. LITERATURE REVIEW	3
Introduction	3
Carbon Fiber Precursors.....	6
Chemistry of Stabilization.....	9
Applications of Carbon Fibers.....	13
Acrylonitrile, Comonomers and Polyacrylonitrile.....	14
Monomers and Comonomers.....	15
Kinetics of Free Radical Addition.....	20
Chain Growth Copolymerization.....	31
Copolymerization Equations.....	36
Determination of Reactivity Ratios.....	39

Chapter III. EXPERIMENTAL.	46
Chemicals, Purification and Reaction Apparatus	46
Copolymerization.	49
Copolymer Isolation	51
Proton Nuclear Magnetic Resonance.	53
Molecular Weight Determination.	57
Real Time Infrared Spectroscopy.	59
Copolymerization Using Real Time Mid-FTIR.	62
Chapter IV. RESULTS AND DISCUSSION.	67
Copolymer Composition Distribution	68
Azeotropic Copolymerizations.	70
Literature Values of Reactivity Ratios.	72
Application of ¹ H NMR to Isolated Copolymers.	72
Reactivity Ratio Determination.	75
Real Time <i>In situ</i> FTIR.	78
Chapter V. CONCLUSIONS.	87
SUGGESTED FUTURE RESEARCH.	90
REFERENCES.	91
VITA	96

List of Figures:

Figure 1: Proposed Chemistry of PAN Stabilization.	9
Figure 2: Benzoyl Peroxide Free Radical Generation.	21
Figure 3: Azobisisobutyronitrile Free Radical Formation.	21
Figure 4: Termination by Combination.	24
Figure 5: Termination by Disproportionation.	24
Figure 6: Thermal Decomposition of AIBN.	48
Figure 7: Reaction Scheme for Copolymerization of AN/MA.	49
Figure 8: ^1H NMR of AN/MA Copolymer.	54
Figure 9: GPC Curve of AN/MA Copolymer.	58
Figure 10: Infrared Absorbance Peaks of AN, MA and DMF	63
Figure 11: Expansion of IR Peaks at 690 and 814 cm^{-1}	64
Figure 12: Waterfall Plot of MA at 814 cm^{-1}	65
Figure 13: AN/MA Monomer Disappearance.	66
Figure 14: Hypothetical Copolymer Composition Change.	69
Figure 15: Illustration of Perfectly Random vs. Azeotropic Copolymerization.	71
Figure 16: Charge vs. Copolymer Compositions for AN	74
Figure 17: Mortimer/Tidwell Reactivity Ratio Plot of Isolated Copolymers	77
Figure 18: Comonomer Feed vs. Copolymer AN Content Using IR Data	84
Figure 19: Reactivity Ratio Plot Using RT-FTIR Data.	86

List of Tables:

Table 1: Modulus of Different Carbon Fibers.	6
Table 2: Applications of Carbon Fiber Composites.	13
Table 3: Amounts of Comonomers, Initiator and Solvent Employed.	51
Table 4: Normalization of Peak Areas.	79
Table 5: Conversion of Normalized Peak Areas to Moles of Monomers	80
Table 6: Conversion of Moles of Monomers to Moles in Copolymers.	81
Table 7: Conversion of Moles of Comonomers to Mole Fractions.	82
Table 8: Conversion of Moles in Copolymers to Mole Fractions.	83
Table 9: Mole Fractions of AN in Feed, Copolymer and Delta F_1	85

Chapter I: Introduction

Polyacrylonitrile is the basis of acrylic fibers,¹ such as well known trade names including Orlon, Acrylan etc., and currently represents about six billion pounds of annual textile product. About thirty million pounds of this product is transformed by complex thermal processes into carbon fiber. Processing of these materials requires solvent based spinning because the homopolymer and the existing random copolymers decompose/cyclize before the crystalline melting point (T_m) at about 300° C. It is envisioned that efficient utilization of comonomers can disrupt the long range order and can allow economical and environmentally attractive melt processing to occur at perhaps 220° C, which is more than 100° C above the glass transition temperature (T_g), while still affording strong fibers.

The objectives of this research were to determine precise, statistically significant reactivity ratios for the homogeneous free radical azoisobutyronitrile (AIBN) initiated acrylonitrile(AN)/methyl acrylate(MA) copolymer formed in N,N-dimethylformamide

(DMF) at low conversion. It was expected that these values should be broadly applicable to other processes such as suspension polymerizations.

The application of proton nuclear magnetic resonance (^1H NMR) was performed on the isolated copolymers at low conversion to determine the copolymer composition. Also, modern real time Fourier Transform infrared spectroscopy (FTIR) was used to provide the copolymer information at low conversions by following the disappearance of the comonomers. Furthermore, the investigation of non-linear methodologies, originally reported by Tidwell and Mortimer², to calculate reactivity ratios was performed with particular focus on the non-linear computer program data reduction method of M.A. van Herk.^{3,4}

Chapter II. Literature Review

INTRODUCTION

Automobile and aerospace structures comprise an important segment of the economy. Fuel efficiency could be greatly improved by the development and commercialization of lightweight, strong polymer matrix composites. Therefore, industry and government agencies such as the Department of Energy are funding research for the development of very strong, lightweight and economically feasible advanced materials such as polymer matrix carbon fiber composites. Although many early efforts focused on military applications for aircraft and space projects, carbon fibers are now being considered for many other uses including automobile body parts, boat hulls and civilian aircraft.

The density of a carbon fiber is relatively low (about 1.8 g/cm^3) and allows high specific strength and modulus relative to other currently available engineering materials. Carbon fibers are quite chemically inert, except for extreme oxidizing conditions or when

in contact with some molten metals. The fibers contribute to low creep and fatigue resistance in composites as well as displaying excellent damping and very good thermo physical properties.

Carbon fibers can be used in different forms to reinforce light-weight thermosetting or thermoplastic organic materials like epoxy resins, polyesters or polyamides. For example, short or continuous yarns, fabrics, etc. can be used to contribute stiffness, strength and reduce the thermal expansion coefficient in the composite.⁵

High performance carbon fiber development started in the 1950's when Union Carbide, now CYTEC FIBERITE, developed a process that produced high modulus fibers by hot stretching of the isotropic pitch based carbon fiber during heat treatment at the graphitisation temperature.⁶ Later, Shindo⁷ in Japan and Watt in the U.K.,⁸ working independently, created carbon fibers from polyacrylonitrile (PAN) precursor fibers. This "black orlon" was prepared from the commercial acrylic fiber that was transformed into high strength carbon fibers by heating it to 200° C for many hours in air, followed by pyrolysis in a flame. A major problem was that the exothermic oxidation reaction to cyclize the fiber needed to be controlled. Watt and Johnson subsequently produced a fiber carbonized at 1000° C, which had a modulus of 150 GPa, which became even higher after further heating at 2500° C. During the early batch process, the need to restrict the fibers during the oxidation process was utilized for the development of a continuous process which featured spinning under tension. By 1966 a full-scale continuous process for converting PAN fiber precursors into carbon fibers was used at Morganite Limited.⁹

The simpler fabrication process and the lower cost in the PAN precursor received immediate attention because the PAN process for carbon fibers was more economical than the rayon (regenerated cellulose) based process. The rayon process used textile grade fibers that were subjected to complicated pyrolysis techniques that obtain a fiber with a carbon yield of only 20%.⁹ The PAN process improved carbon fiber yields (50%) relative to the rayon process and did not require the expensive and difficult high temperature orientation. The PAN precursor needed for high performance had to have a preferred orientation but stretching the fiber when it was still relatively thermoplastic sufficed. The orientation helped to compensate for the shrinkage when the fiber was cyclized into the more stable infusible acrylic fiber when heat-treated in air at 200° C. Further carbonization, at 1200-1400° C, of the stabilized fiber helped to increase the tensile strength to about 3.0 GPa and the modulus to about 250 GPa. Further post carbonization at 2500° C, improved the modulus to 350 GPa, but the tensile strength decreased.

The process development in the carbon fiber industry could, in principle, be applied to light weight automobile parts that would reduce energy consumption. Therefore, many types of precursors are under investigation to test the feasibility for a large-scale economical production route to carbon fibers.¹⁰⁻¹⁵

Different classifications of carbon fibers exist and although new grades of carbon fibers with enhanced physical properties are being produced, certain classifications have been generically set. Table 1 shows one view of modulus and approximate tensile strength-to-tensile modulus values that are believed to be feasible.

UHM Type	Carbon fibers with modulus greater than 500 GPa.
HM Type	Carbon fibers with modulus greater than 300 GPa and with a tensile-strength and tensile to modulus ratio of less than 1%.
IM Type	Carbon fibers with modulus up to 300 GPa and with a strength to modulus ratio above 1×10^{-2} .
Low Modulus Type	Carbon fibers with modulus as low as 100 GPa and with low strength. Carbon fibers that have an isotropic structure.
HT Type	Carbon fibers with tensile strength values greater than 3000 MPa and strength to stiffness ratio between 1.5 and 2×10^{-2} .

Table 1: Moduli of different types of carbon fibers. Reprinted from IUPAC international committee on nomenclature and characterization of Carbons and Graphite.¹⁶

It becomes apparent that the properties of carbon fibers can be varied dramatically by changing the process parameters such as the final heat treatment temperature and the type of precursor material.

CARBON FIBER PRECURSORS

Rayon (regenerated cellulose from viscose), PAN, aromatic heterocyclic polymers and pitch based precursor fibers are examples of several organic materials that have been investigated for the preparation of carbon fibers. Mainly, large scale production of carbon fibers only uses three of these starting materials: PAN (including copolymers), pitch and rayon precursor fibers. Polyacrylonitrile (PAN) based precursor fibers are the most important groups of precursors. The PAN fibers are highly desirable for high performance composites for automobiles and aerospace technologies due to their

enhanced physical and mechanical characteristics. The pitch-based carbon fibers are useful because of the lower price (in principle) of production and the unique structural characteristics like orientation and modulus. Rayon based carbon fibers contain lower fractions of carbon where the carbon yield is very low at 15-20%. The processing of high performance materials made from regenerated cellulose rayon fibers requires difficult and expensive high temperature heat treatments. Therefore, the production of carbon fibers from rayon fibers is very restricted.¹⁶

The pyrolytic manufacturing of carbon fibers requires similar steps for all the types of precursors. The first step after organic fiber formation is to “stabilize” the material in order to restrict melting or fusion of the fibers. The second step involves a carbonizing heat treatment of the stabilized fiber to remove the non-carbon elements. The third step is to further heat treat the fiber at a higher graphitization temperature in order to increase the mechanical properties. The degree of orientation determines some mechanical characteristics in the final carbon fiber and requires that the precursor fibers be given a stretch treatment during one of the processing steps. For the pitch fibers, this orientation step is carried out during the spinning stage. For the PAN fibers, the stretching is done during the oxidative stabilization step. The rayon based fiber orientation is produced during the high temperature treatment.

Present day carbon fibers are mainly produced from PAN based acrylic fibers. PAN fibers have a high degree of orientation, a high (~300° C) melting point and produce a carbon fiber of relatively high carbon yield (50%). The PAN fibers give rise to a thermally stable, extremely oriented molecular structure when subjected to a low

temperature treatment. Furthermore, during the carbonization treatment at a much higher temperature, the highly oriented molecular structure is not significantly disrupted.¹⁶

The major comonomer currently used in the production of the PAN precursor is methyl acrylate. There is often present a third comonomer such as itaconic acid that helps to initiate the “stabilization” reaction at the lower temperature. The use of the comonomer disrupts the long range ordering of the polyacrylonitrile, which increases the solubility, decreases the crystallinity and increases the cyclization temperature. This facilitates the spinning process and the further stretching of the fiber during the oxidative stabilization. Orientation of the fiber increases the length by about 15 times.⁹ This helps to align the molecular chains along the fiber axis; this further enhances the mechanical characteristics of the carbon fibers.

The normal temperature for the oxidative stabilization is 200-300° C. A constant load is applied to the fiber and the atmosphere is usually air. The chemistry of the stabilization process is complex, but consists of intramolecular cyclization and crosslinking of the chain molecules followed by dehydrogenation and oxidative reactions. This process transforms the linear polymer into a more thermally stable cyclized structure. Figure 1 shows how the pendent nitrile groups of the PAN may cyclize to produce heterocyclic structures.

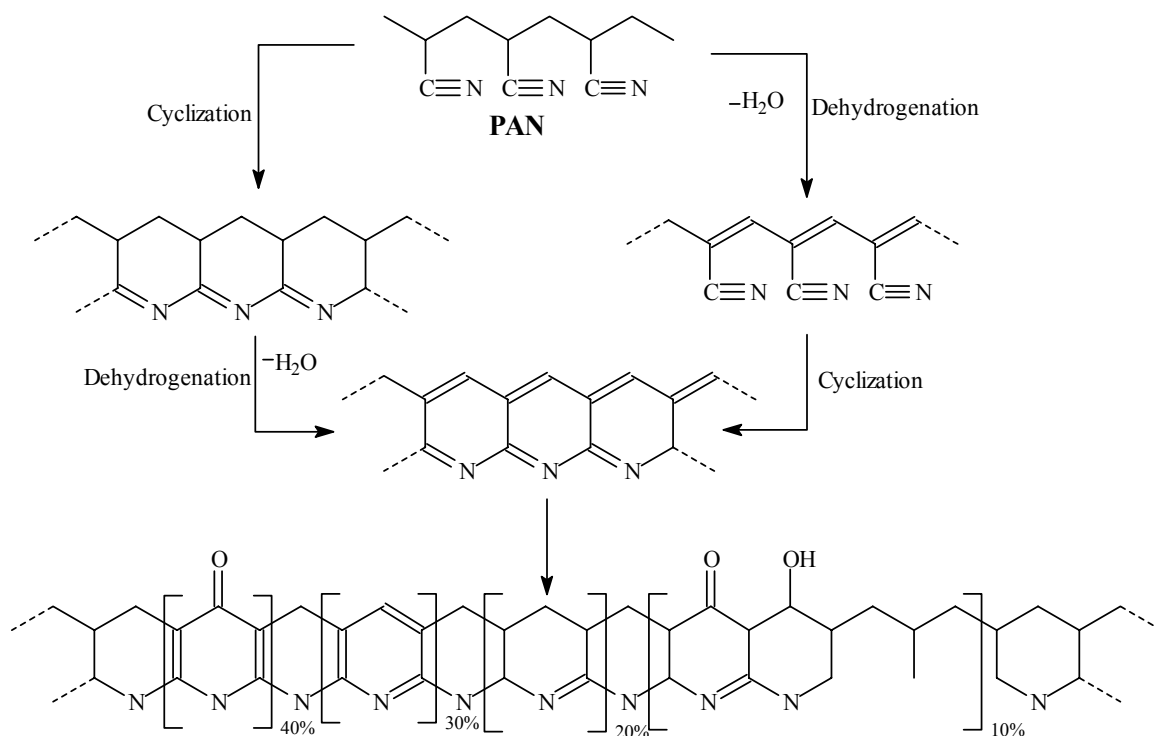


Figure 1: Proposed Chemistry of PAN stabilization⁹

The formation of the stabilized polymer and the evolution of volatiles such as H₂O, CO₂ and HCN are observed during the reaction. Between 8-10% oxygen still remains in the “stabilized” polymer in the form of ketone and hydroxyl groups. These reactive groups may further induce intermolecular crosslinking. More than 12% oxygen in the stabilized copolymer has been noted to result in a fiber that is of poor quality mechanically and less than 8% results in a low carbon content that appears to correlate with high weight loss during the further carbonization process.⁹

The oxidative stabilization causes a shrinking of up to a third of the overall dimensions of the fiber. The shrinkage is accounted for by the chemical cyclization

crosslinking and the dehydrogenation reactions and further by the molecular relaxation.¹⁷ By 200° C the relaxation shrinkage is completed and chemical shrinkage becomes more important. The shrinkage due to relaxation above T_g can be decreased by either restraining the fiber under a constant force or in a longitudinal direction during the “stabilization” heat treatment.

After the PAN fibers are stabilized, they are next thermally pyrolysed in an inert atmosphere where the non-carbon elements are removed as volatiles. This process produces up to a 50% carbon yield of carbon fiber when PAN homopolymer is used. The first stage of thermal pyrolysis at 300-600° C involves chemical reactions that produce HCN, CO₂, NH₃ and H₂O as volatiles and also hydrocarbons in the form of tar. The degree of stabilization of the PAN fiber correlates with the amount of tar that is produced. The rate of volatile evolution depends on the heating rate, which is kept low (about 1.5° C/min). Damaged fiber results if the volatiles are removed too fast; low carbon content is the result of a large amount of tar being produced. Also during the first stage, the oxygen containing groups are proposed to initiate the crosslinking condensation reactions that produce a fixed structure, while other linear segments become cyclised or undergo chain scission. The second stage of the thermal pyrolysis is done at 600-1300° C and consists of the cyclised structures undergoing dehydrogenation as well as linking in the lateral directions. The oriented heterocyclic molecules become graphite like and evolve nitrogen and hydrogen. Up to 50% carbon yield after the pyrolysis can reportedly be enhanced by carbonizing in an atmosphere of hydrochloric acid vapors. The third and final stage of the pyrolysis is done at 1300-2500° C, the graphitization temperature. Improved orientation of the crystallites in the direction of the fiber axis, without any

noticeable weight loss, is achieved by the heat treatment (a few seconds). The enhanced mechanical properties produces a high performance carbon fiber suitable for many applications.¹⁸

Many properties such as high specific strength and stiffness, light-weight, chemical inertness, thermal and electrical compatibility and vibrational characteristics of carbon fibers make them an extremely versatile material. However, some problems are that at low extension the fibers fracture and do not have good impact resistance. The high cost of these fibers limits the use of carbon fibers to high technology applications where the cost is not the main issue. The recent focus has been to find ways to reduce cost and to increase the number of applications, especially for autos.

Two main areas where carbon fibers are used today are in aerospace and nuclear engineering. The secondary area is in the general transportation and engineering sector. The latter is where the fibers are used for such things as camshafts, fan blades, bearings and automobile bodies. The needs of these two sectors are different; high technology applications like aerospace and aircraft need the carbon fibers for maximum fuel efficiency and performance with less concern for low cost. In contrast, the general engineering carbon fibers must be cost competitive with other materials that have some of the same characteristics. The acceptable matrices, material forms and manufacturing methods need to be focused on in order to understand the differences in the two areas of carbon fiber use.

Unidirectional anisotropic reinforcement is a characteristic of carbon fibers. Essentially the fibers can be arranged in such a way that the material produced is much stronger in one direction, where it must bear loads. The general requirements of the

materials are complex, because the structures need to bear loads, resist deflection and give high performance in more than one direction. Furthermore, operation under different mechanical, physical and chemical environments is important. In order to make the material bear loads in more than one direction, the fibers need to be arranged in layers comprising more than one direction to have better efficiency. Designers are able to selectively change these layered arrays in order to fit the specific needs of the reinforced materials. The use of more than one reinforcement material in a certain application is being realized, because there is no one fiber that can be used for all the economical and technical requirements. Therefore, a development of a variety of reinforcement fibers that have different mechanical, electrical and physical properties is leading the way in expanding carbon fiber technology. The use of Kevlar as a second reinforcement material with carbon fibers can provide the composite material with better impact strength than carbon fiber alone and better compressive strength than with Kevlar alone. These hybrid fibers, where more than one reinforcement fiber is used, can consist of glass fibers, boron fibers, Kevlar fibers and carbon fibers, etc. Differences in this hybridization within a matrix can consist of using two or more fibers in the same fabric, called intraply hybrid, or one can mix the fiber plies through the composite cross section, called interply hybrid.⁹ Table 2 indicates some applications of carbon fiber composites on the basis of their most significant mechanical and physical properties.

Physical strength, specific toughness, light weight	Aerospace, road and marine transport, sporting goods
High dimensional stability, low coefficient of thermal expansion, and low abrasion	Missiles, aircraft brakes, aerospace antenna and support structures, large telescopes, optical benches, waveguides for high-frequency (GHz) precision measurement frames
Good vibration damping, strength and toughness	Audio equipment, loudspeakers for Hi-Fi equipment, pickup arms, robot arms
Electrical conductivity	Automobile hoods, novel tooling, casings and bases for electronic equipments, EMI and RF shielding, brushes
Biological inertness and X-ray permeability	Medical application in prostheses, surgery and X-ray equipment, implants, tendon/ligament repair
Fatigue resistance, self-lubrication, high damping	Textile machinery, general engineering
Chemical inertness, high corrosion resistance	Chemical industry; nuclear field; valves, seals and pump components in process plants
Electromagnetic properties	Large generator retaining rings, radiological equipment

Table 2: Application of carbon fiber composites on the basis of their most significant mechanical and physical properties⁹

High specific strength, stiffness and lighter weight materials are the common themes in all the applications of carbon fibers. As compared to steel, the composites made have superior mechanical properties and are lighter in weight by 45-75%. Many other physical properties of carbon fibers, like thermal conductivity and corrosion resistance, can be optimized by changing the matrix material and the processing conditions for the production of the carbon fibers or reinforced polymer matrix composite (PMC).

ACRYLONITRILE BASED COPOLYMERS AND FIBERS

Japan has recently been the leading contributor in the diversification of the production of modified acrylic fibers.¹⁹ Characteristics such as high tenacity, low elongation, permanently soft lustrous, micro porous, antistatic, acid dyable, water resistant, and flame resistant fibers are all examples of currently available new acrylic fibers. These new high performance acrylic based fibers are used in the civil and engineering field for applications like composite materials, a substitute for asbestos, hollow ion exchange fibers and precursors for high strength carbon fibers.

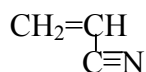
As compared to textile grade acrylic fibers, high performance acrylic fibers need extremely stringent control during production. The physical and chemical properties of these structures are greatly influenced by the chemical composition, molecular weight, molecular weight distribution, spinning and post spinning parameters. More than 85% of acrylonitrile monomer must be incorporated into the copolymer in order for it to be termed an acrylic fiber.

Copolymerization of acrylonitrile with various comonomers produces specialty fibers for different applications. The homopolymer of acrylonitrile, PAN, has inferior properties in carbon fibers when compared to PAN copolymers. Enhanced mobility of polymer segments, or decrease in the glass transition temperature (T_g), generally occurs when only a small percentage of a comonomer is used. The interactions of the comonomers help to depress the onset of the cyclization temperature during oxidation and improve the spinnability. Furthermore, increased comonomer concentration in the PAN decreases the crystallinity and the crystallite size.

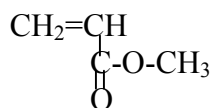
The manufacturing of acrylic fibers requires a copolymer with some dye sites, specific molecular weight and controlled composition. Therefore, the copolymerization process is obviously an extremely important step in the overall manufacturing of the fibers. Acrylic fibers are always made with acrylonitrile and at least one or two comonomers. Either neutral and/or ionic comonomers can be employed.

Methyl acrylate (MA), methyl methacrylate (MMA) and vinyl acetate (VA) are the commonly used “neutral” comonomers. They increase solubility and change the morphology of the fiber. Comonomers also improve the rate of diffusion of the dye into the fiber. The amounts of neutral comonomers in commercial acrylic fibers are from 2-15 mole percent or 5-20 weight percent. When dry spinning the polymer, MA is used because VA reduces the stability of the spinning dope at increased temperatures in the spinning tower.²⁰⁻²²

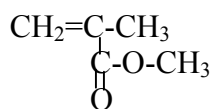
Acrylonitrile (AN)



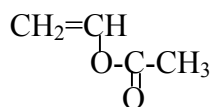
Methyl Acrylate (MA)



Methyl Methacrylate (MMA)



Vinyl Acetate (VA)

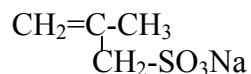


Sodium-p-styrene sulphonate, sodium methallyl sulphonate and sodium 2-methyl-2-acrylamido-propane sulphonate are examples of ionic comonomers probably used in

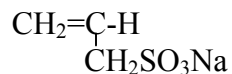
the polymerization process. They all provide dye sites and improve water sorption.

Around 30-50 meq kg⁻¹ of sulphonate and sulphate dye sites are needed for acrylic fibers that are colored with cationic dyes.²¹

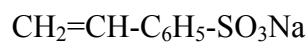
Sodium Methallyl Sulphonate (SMS)



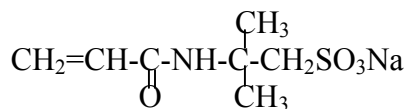
Sodium Allyl Sulphonate (SAS)



Sodium Styrene Sulphonate (SSS)



Sodium 2- acrylamido -2- methyl -
propane Sulphonate (AMPS)



Several methods for polymerization have been successfully used to make homo and copolymers of acrylonitrile, including solution, suspension and emulsion polymerizations.²¹ Solution polymerization is the most widely used technique to produce acrylic polymer fibers. Both homo and copolymers of acrylonitrile use this method because it has the advantage that one can spin the polymer directly after the polymerization process. The unreacted monomers must of course, be removed and the spinning dope viscosity needs to be controlled. Usually a homogeneous medium is used for the reaction and solvents such as N,N-dimethylformamide (DMF), dimethylacetamide (DMAc) and dimethyl sulphoxide (DMSO), are generally used. To initiate the reaction, thermally activated free radical initiators like azobisisobutyronitrile (AIBN) and redox systems like ammonium persulfate and sodium persulfate can be employed. Anionic and

free radical initiators are the only means to accomplish initiation of polymerization of acrylonitrile. Anionic polymerization involves nucleophilic addition to the vinyl group but it may also attack the nitrile group, which is obviously not desired.

Although solution polymerization is advantageous as discussed above, there are limitations. Comonomers such as vinyl acetate and vinyl chloride are not easily used because of undesirable reactivity ratios and inferior color in the resulting polymer. In order to dry-spin the polymer, a solvent that has a relatively high boiling point must be used and the choice is usually DMF.²³

Suspension polymerization is another very important technique used to produce acrylic fibers. Aqueous suspension polymerization uses water as a convenient medium for heat transfer and the polymer is very easy to recover by simple filtration. Solvent-water suspension polymerization is a technique where water is used with solvent in about the same proportions by weight at the beginning of the reaction. Later during polymerization, more water is added to reduce chain transfer due to the solvent.

Inorganic radical generators, like persulfates, and organic initiators, like AIBN, are used in suspension polymerization.²⁴ Ammonium or potassium persulfates as oxidizers and sodium bisulfite as a reducing agent are the most common redox systems used. The kinetics are similar for that of solution and suspension polymerizations, but termination is usually by radical recombination in suspension systems. The chemical and physical properties of the polymer, such as molecular weight and dye sites, vary according to solvent/monomer ratio, bisulfite/persulfate ratio, reactor temperature, pH of reactor slurry, addition of chain stopping agents and agitator speed.

Thus, wet and dry spinning are the techniques that are most often used for the production of acrylic fibers. Melt spinning is not yet possible because the acrylic precursor will degrade before it reaches its melting point. Melt processing can be accomplished by adding comonomers that decrease or eliminate the melting point, T_m . The T_m may also be depressed by the use of plasticizers, solvents and the addition of water under pressure. It has been reported that under pressure the polymer-water mixture can hydrate the nitrile groups which allows the melt to be extruded.²⁴

The wet spinning process uses a spinning dope that is extruded through a multi-hole spinneret into a non-solvent coagulation bath. After the dope jets coagulate into solid filaments and are then removed from the spinning bath, they are washed in hot water to remove the rest of the solvent. Then the fiber is drawn and subjected to drying, crimping and annealing. The linear speed of the fiber formation by solution spinning is extremely slow in comparison to melt spinning. Therefore, to obtain an economically feasible productivity, many spinnerets having multiple thousands of holes are used. Then, the filaments from many spinnerets are combined to make the required denier.

The dope preparation is done in a variety of solvents and the polymer concentration is dependent upon which solvent is used. Usually the concentration ranges from 10-25% solids. Solution polymerization dope uses the same solvent as the polymerization process. Aqueous slurry (suspension) polymerization recovers the polymer by filtration to form a wet polymer cake. Therefore, the spinning dope solution is an aqueous salt solution where the polymer cake can be dissolved directly.²⁵

Fiber extrusion is performed by degassing the filtered dope that contains 10-25 weight percent polymers and spinning it through spinnerets with 10,000-60,000 holes,

which can range from 0.05 to 0.38 mm in diameter. The fiber is then strung into a liquid bath that contains a non-solvent for the polymer. After the solvent is removed, fiber formation happens rapidly during the coagulation of the polymer material.

Dry spinning is the other common technique used to produce acrylic fibers for industrial goods. The dope solution contains a higher amount of polymer, 30-32% by weight. Furthermore, the rate of dry spinning is much faster than that of the rate for wet spinning, e.g. 200-400 meters per minute and 3-10 meters per minute respectively. The extrusion process uses a spinneret with only 1500-2500 holes, which is put at the head of a two chamber vertical tower that is 5-6 meters high. In the tower, there is inert gas that is preheated to 300-400° C. The upper cell of the tower contains inert gas, such as nitrogen, at 350-400° C that flows from top to bottom removing the solvent. The solvent is recovered by distillation and the gas is then recycled after being heated back up. The lower column uses a lower temperature that helps to cool the fiber bundle and also removes more solvent. The solvent is once again removed from the gas by distillation and the gas is then recycled after pre-heating. The fibers that leave the two-column tower may still contain 10-20% solvent. In comparison, the dry spinning process is more expensive because of the systems needed in the column. The gas circulation, the solvent recovery techniques and the heating are all expensive processes. The comparison of the fibers using DMF as the solvent shows that the dry spun fibers have higher bulkiness and can recover from deformation better. The wet spun fibers are softer and fleecier and have a better dye pick-up. The wet spinning process is recommended when a low denier fiber, fineness of thread, is needed, 1.2-3.0 denier (grams per 9000 meters).²¹

The high price of solution and suspension acrylic fibers has made the industries interested in more economical ways to produce the fibers. The high cost mainly comes from the use and disposal of the solvent, but also comes from the slower rates of processing and the expensive equipment needed for processing. Thus, the aqueous dispersion copolymerization of acrylonitriles and acrylates would be expected to decrease the cost for solvents and decrease the environmental impact of the disposal of these solvents. Furthermore, the development of melt-spinnable PAN copolymers would be expected to reduce the cost by increasing the rate and ease of processing at comparable volumes.

KINETICS OF FREE RADICAL ADDITION: Homo and Copolymerization

Understanding of chemical kinetics during homo- and copolymerization is crucial for copolymer synthesis. The discussion below will review the kinetics of free radical initiated polymerizations and copolymerizations.

The three main kinetic steps that occur during polymerization are (1) initiation, (2) propagation, and (3) termination. Chain transfer is also important. Many methods can be used to initiate free radical polymerizations, such as thermal initiation without added initiator, or high energy radiation of the monomers. However, free radicals are usually generated by the addition of initiators that form radicals when heated or irradiated. Two common examples of such compounds which afford free radicals are benzoyl peroxide (BPO) and azobisisobutyronitrile (AIBN).

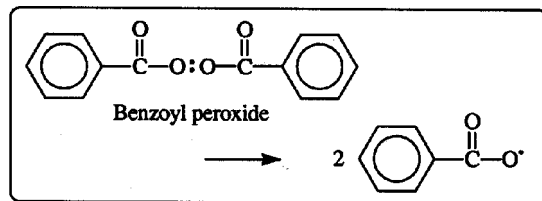


Figure 2: Generation of Free Radicals by Thermal Decomposition of Benzoyl Peroxide

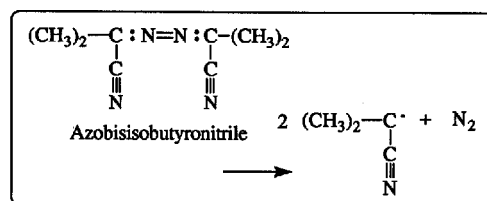


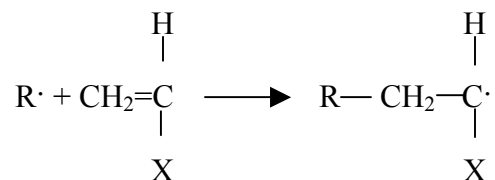
Figure 3: Decomposition of Azobisisobutyronitrile to Form Free Radicals

Figure 2 depicts the thermal decomposition of BPO to form two oxy-radicals and Figure 3 depicts the decomposition of AIBN to form two nitrile stabilized carbon based radicals (equation 1):

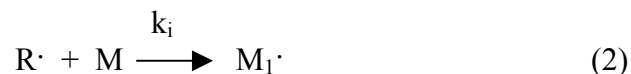


In equation 1, k_d is the rate constant which describes the first order initiation process.

The radical that is formed can now add to the double bond of the monomer and initiate polymerization:



The symbol M will represent the monomer and the rate constant for this process will be k_i , as described in equation 2:



Together, these two reactions, the radical generation and the monomer addition to the radical, form the process of initiation. Usually, the assumption that is taken into account is that the first step is the rate determining step. This means that the decomposition to form the radical is much slower than the monomer addition to the free radical. Therefore, the equation for the rate of radical formation, r_i , is:

$$r_i = \frac{d[M_1\cdot]}{dt} = 2 k_d [I] \quad (3)$$

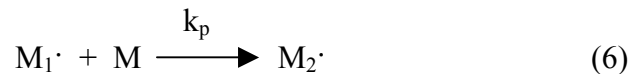
The number 2 is obtained from the fact that a maximum of two radicals can be generated for the initiation:

$$-\frac{d[I]}{dt} = \frac{1}{2} \frac{d[M_1\cdot]}{dt} = k_d [I] \quad (4)$$

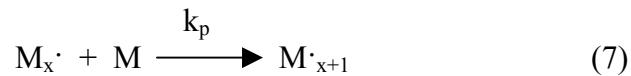
But, not all of the primary radicals produced by the decomposition of the initiator will necessarily react with the monomer, which means several other competing reactions may occur.²⁶ Therefore, in order to determine the rate of initiation, the fraction of initially formed radicals that actually start chain growth will be denoted by f , and the rate of initiation equation becomes:

$$r_i = \frac{d[M_1\cdot]}{dt} = 2 f k_d [I] \quad (5)$$

Now, the propagation of the reaction will proceed through the successive addition of monomer to the radicals. This type of process can be expressed in the following form:



And further generalizing the reaction scheme gives:



The assumption that the reactivity of the addition of each monomer is independent of the chain length is evident in these two equations and was postulated by Flory.^{27,28} The use of the rate constant, k_p , for both of these equations imply that the rate constant is independent of chain length. The rate of the propagation, r_p , of this polymerization, or the rate of monomer removal, is thus given by:

$$r_p = - \frac{d[M]}{dt} = k_p [M\cdot] [M] \quad (8)$$

The termination of these growing radical chains occurs in principally two different ways. The first way is the formation of a new bond in between the two radicals; this is called combination. Secondly, the radical chains can terminate by disproportionation. This is a process where a hydrogen atom from one of the chains is

transferred to the other and the chain that the proton was removed from forms a double bond. These reactions are represented as follows:

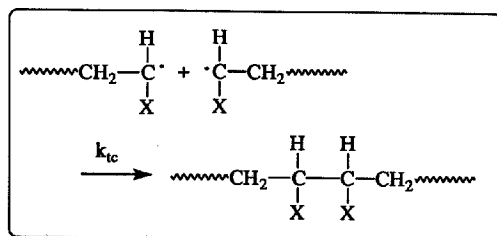


Figure 4: Termination by Combination

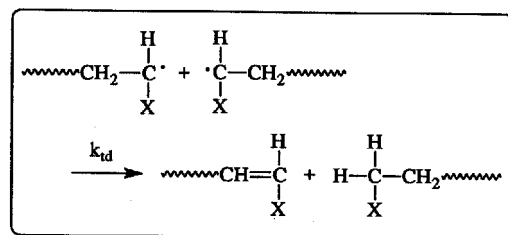


Figure 5: Termination by Disproportionation

Schematically, the reactions can be represented as follows:



Where the rate constant of termination by combination is denoted by k_{tc} , and the rate constant of termination by disproportionation is denoted by k_{td} . Since both of these reactions use two radical species and have the same kinetics, the overall equation for the rate of termination is written as:

$$r_t = - \frac{d[M\cdot]}{dt} = 2k_t [M\cdot]^2 \quad (11)$$

where $k_t = k_{tc} + k_{td}$ and the number 2 imply there are two radicals that are terminated in each termination reaction. The monomer structure and the temperature are what determines the type of termination that is most dominant in the reaction. For most systems, the amount of one termination type far exceeds the other termination type.

The further calculations for the rate of polymerization, R_p , and the degree of conversion as a function of time can now be developed. The assumption of the steady state concentration of transient species must be used here, where the transient species is the radical $M\cdot$. For the steady state approximation to hold true, the rate at which initiation occurs, r_i , must be equal to the rate at which termination occurs, r_t , or in other words, radicals must be generated at the same rate at which they are terminated. This assumption gives the equation:

$$2 f k_d [I] = 2 k_t [M\cdot]^2 \quad (12)$$

This equation then gives an expression for the radical species:

$$[M\cdot] = [(f k_d [I]) / (k_t)]^{1/2} \quad (13)$$

Experimentally, this value would be difficult to measure in the laboratory, and therefore, this equation must be used in the subsequent equations that follow. By further

substitution, an expression for the rate of polymerization, R_p , can be obtained because it equals the rate of propagation:

$$R_p = - \frac{d[M]}{dt} = k_p \left(\frac{f k_d [I]}{k_t} \right)^{1/2} [M] \quad (14)$$

From this equation, it can be deduced that the rate of polymerization is directly proportional to the monomer concentration and to the initiator concentration to the one half power. In other words, R_p is first order with regards to the monomer concentration and half order to the initiator concentration.

When the conversion is low, the assumption that the initiator concentration is constant is reasonable, but the consumption of the initiator can be added into the calculations. Therefore:

$$\frac{d[I]}{dt} = -k_d [I] \quad (15)$$

Then, integration can be performed:

$$[I] = [I]_0 e^{-k_d t} \quad (16)$$

Finally the rate of polymerization becomes:

$$R_p = \left\{ k_p \left(\frac{f k_d}{k_t} \right)^{1/2} \right\} \left\{ [I]_0^{1/2} [M] \right\} e^{-k_d t / 2} \quad (17)$$

This equation can be broken into three different parts.

The second term indicates that the rate of polymerization is still proportional to the monomer concentration to the first power and the initiator concentration to the one half power, but the initiator concentration is now the initial concentration. Therefore, by increasing the initial concentration of an initiator in a solution polymerization, the rate of the reaction should increase proportionally to the square root of the amount of initiator added.

The third term indicates that as the initiator is consumed, the polymerization slows down exponentially with time as well as its slowing down due to monomer depletion.

The first term in the brackets suggests that the rate of polymerization is proportional to $k_p / k_t^{1/2}$. When experiments are performed to probe the kinetics of reactions in solution, the expected first order dependence on monomer concentration is observed. But, when the experiment is performed in concentrated solvents or even in the bulk, the polymerization kinetics accelerate. The reason for this anomaly is that the viscosity increases as the polymerization proceeds because the polymer has a higher viscosity than the monomers. The k_p is not affected, but the k_t is.

The degree of conversion can now be expressed as a function of time by knowing that:

$$R_p = - \frac{d[M]}{dt} \quad (18)$$

By substituting the earlier equation for R_p and integrating that equation, one can obtain this:

$$\ln \frac{[M]_0}{[M]} = 2 k_p \left(\frac{f k_d}{k_t} \right)^{1/2} [I]_0^{1/2} \left(1 - e^{-k_d t / 2} \right) \quad (19)$$

Furthermore, $([M]_0 - [M]) / [M]_0$ is equal to the degree of conversion and is the fraction of the monomer that has been reacted, where $[M]$ is the concentration of the monomer that has been left after the reaction and $[M]_0$ is the initial monomer concentration. Therefore, $([M]_0 - [M])$ is the concentration of the monomer that has reacted. The conversion can then be expressed as:

$$\text{Fractional conversion} = \frac{[M]_0 - [M]}{[M]_0} = 1 - \frac{[M]}{[M]_0} \quad (20)$$

Which can also be expressed as:

$$\text{Conversion} = 1 - \exp - \left\{ 2 k_p \left(\frac{f k_d}{k_t} \right)^{1/2} [I]_0^{1/2} \left(1 - e^{-k_d t / 2} \right) \right\} \quad (21)$$

As is always the case, the conversion never quite reaches 100% value or a factor of 1 given by the exponential term. So, if the time goes to infinity, the expression that is obtained for maximum conversion that is less than 1 by an amount that is dependent on the initial initiator concentration is:

$$\text{Maximum Conversion} = 1 - \exp - \left\{ 2 k_p \left(\frac{f k_d}{k_t} \right)^{1/2} [I]_0^{1/2} \right\} \quad (22)$$

If the steady state approximation for the initiator concentration had been carried through these calculations and equations, then the conversion would approach a value of 1 after a long period of time.

Distributions on the average distribution of chain lengths during and after a polymerization are present in free radical polymerizations. This is due to the naturally but statistically random termination reactions that occur in the solution with regard to chain length. The kinetic chain length, ν , is the rate of monomer addition to growing chains over the rate at which chains are started by radicals, which is the expression for the number average chain length. In other words, it is the average number of monomer units per growing chain radical at a certain instant.²⁹ Therefore, the initiator radical efficiency in polymerizing the monomers is:

$$\nu = \frac{r_p}{r_i} = \frac{k_p [M]}{2 (f k_d k_t)^{1/2} [I]^{1/2}} \quad (23)$$

When termination occurs mainly by combination, the chain length for the polymer chains, on the average, doubles in size, assuming nearly equal length chains combine. But if disproportionation mainly occurs, the growing chains do not undergo any change in chain length during the process. So, the expressions are thus:

$$\bar{x}_n = 2\nu \quad (\text{termination by combination}) \quad (24)$$

$$\bar{x}_n = v \quad (\text{termination by disproportionation}) \quad (25)$$

A new term can be used to more generally express the average chain length of the growing polymer chain, \bar{x}_n . This new term is the average number of dead chains produced per termination, ξ . This value is equal to the rate of dead chain formation over the rate of the termination reactions. The equations that can thus be written take into account that in combination only one dead chain is produced and in disproportionation reactions two dead chains are produced. Therefore:

$$\text{Rate of dead chain formation} = (2 k_{td} + k_{tc}) [M\cdot]^2 \quad (26)$$

$$\text{Rate of termination reactions} = (k_{tc} + k_{td}) [M\cdot]^2 \quad (27)$$

$$\xi = \frac{k_{tc} + 2 k_{td}}{k_{tc} + k_{td}} = \frac{k_{tc} + 2 k_{td}}{k_t} \quad (28)$$

Furthermore, the instantaneous number average chain length can be expressed in terms of the rate of addition of the monomer units divided by the rate of dead polymers forming. This is shown as:

$$x_n = \frac{k_p [M\cdot] [M]}{(2 k_{td} + k_{tc}) [M\cdot]^2} = \frac{k_p [M]}{\xi (f k_d k_t)^{1/2} [I]^{1/2}} \quad (29)$$

From this equation,²⁹ one can clearly see that the rate of polymerization is proportional to the initiator concentration to the one half power, $[I]^{1/2}$, and that the instantaneous number average chain length, \bar{x}_n , is proportional to the inverse of the initiator concentration to the one half power, $1/[I]^{1/2}$. Thus, if the polymerization was

accelerated by using more initiator, the chains will end up to be shorter, which may not be desirable.²⁶

CHAIN GROWTH COPOLYMERIZATION

Chain polymerizations can obviously be performed with mixtures of monomers rather than with only one monomer. For many free radical polymerizations, for example acrylonitrile and methyl acrylate, two monomers are used in the process and the subsequent copolymer might be expected to contain both of the structures in the chain. This type of reaction that employs two comonomers is a copolymerization. The reactivity and the relative concentrations of the two monomers should determine the concentration of each comonomer that is incorporated into the copolymer.

The application of chain copolymerizations has produced much important fundamental information. Most of the knowledge of the reactivities of monomers via carbocations, free radicals, and carbanions in chain polymerizations has been derived from chain copolymerization studies. The chemical structure of these monomers strongly influences reactivity during copolymerization. Furthermore, from the technological viewpoint, copolymerization has been critical to the design of the copolymer product with a variety of specifically desired properties. As compared to homopolymers, the synthesis of copolymers can produce an unlimited number of different sequential arrangements where the changes in relative amounts and chemical structures of the monomers produce materials of varying chemical and physical properties.

Several different types of copolymers are known and the process of copolymerization can often be changed in order to obtain these structures. A statistical or random copolymer may obey some type of statistical law which relates to the distribution of each type of comonomer that has been incorporated into the copolymer, Thus, for example, it may follow zero- or first- or second-order Markov statistics.¹ Copolymers that are formed via a zero-order Markov process, or Bernoullian, contain two monomer structures that are randomly distributed and could be termed random copolymers:



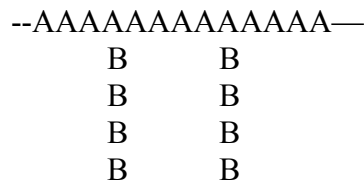
Alternating, block and graft copolymers are the other three types of copolymer structures. Equimolar compositions with a regularly alternating distribution of monomer units are alternating copolymers:



A linear copolymer that contains one or more long uninterrupted sequences of each of the comonomer species is a block copolymer:



A graft copolymer contains a linear chain of one type of monomer structure and one or more side chains that consist of linear chains of another monomer structure

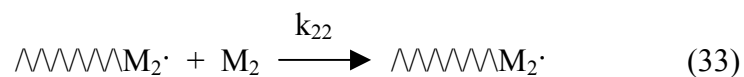
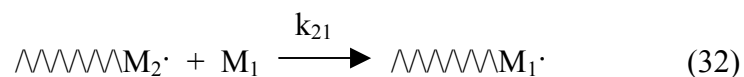
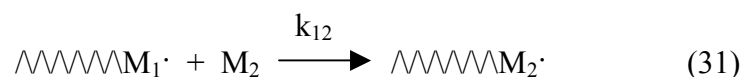
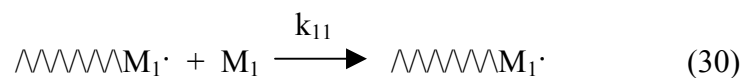


For this discussion, the main focus will be on randomly distributed or statistical copolymers.

Copolymer composition is usually different than the composition of the starting materials charged into the system. Therefore, monomers have different tendencies to be incorporated into the copolymer, which also means that each type of comonomer reacts at different rates with the two free radical species present. Even in the early work by Staudinger,³⁰ it was noted that the copolymer that was formed had almost no similar characteristics to these of the homopolymers derived from each of the monomers. Furthermore, the relative reactivities of monomers in a copolymerization were also quite different from their reactivities in the homopolymerization. Thus, some monomers were more reactive while some were less reactive during copolymerization than during their homopolymerizations. Even more interesting was that some monomers that would not polymerize at all during homopolymerization would copolymerize relatively well with a second monomer to form copolymers. It was concluded that the homopolymerization features do not easily directly relate to those of the copolymerization.

Alfrey(1944), Mayo and Lewis(1944) and Walling(1957),³¹⁻³³ demonstrated that the copolymerization composition can be determined by the chemical reactivity of the free radical propagating chain terminal unit during copolymerization. Application of the first-order Markov statistics was used and the terminal model of copolymerization was proposed. The use of two monomers, M_1 and M_2 , during copolymerization leads to two types of propagating species. The first of these species is a propagating chain that ends with a monomer of structure M_1 and the second species is a propagating chain that ends with a monomer structure M_2 . For radically initiated copolymerizations, the two structures can be represented by $\sim\sim\sim\sim M_1\cdot$ and $\sim\sim\sim\sim M_2\cdot$, where the zig-zag lines represent the chain and the $M\cdot$ represents the radical at the growing end of the chain. The

assumption that the reactivity of these propagating species only depends on the monomer unit at the end of the chain is called the terminal unit model.²⁷ If this is so, only four propagation reactions are possible for a two monomer system. The propagating chain that ends in $M_1\cdot$ can either add a monomer of type M_1 or of type M_2 . Also, the propagating chain that ends in $M_2\cdot$ can add a monomer unit of type M_2 or of type M_1 . Therefore, these equations can be written with the rate constants of reactions:³⁴



The rate constant for the reaction of the propagating chain that ends in M_1 and adds another M_1 to the end of the chain is k_{11} , and the rate constant for the reaction of the propagating chain that ends in M_2 and adds M_1 to the end of the chain is k_{21} , and so on. The term self-propagation refers to the addition of a monomer unit to the chain that ends with the same monomer unit and the term cross-propagation refers to a monomer unit that is added the end of a propagating chain that ends in the different monomer unit. These (normally) irreversible reactions can propagate by free radical, anionic or cationic processes, although active lifetimes could be very different.

As indicated by reactions 30 and 32, monomer M_1 is consumed and as indicated by reactions 31 and 33, monomer M_2 is consumed. The rates of entry into the copolymer and the rates of disappearance of the two monomers are given by:

$$-\frac{d[M_1]}{dt} = k_{11} [M_1 \cdot] [M_1] + k_{21} [M_2 \cdot] [M_1] \quad (34)$$

$$-\frac{d[M_2]}{dt} = k_{12} [M_1 \cdot] [M_2] + k_{22} [M_2 \cdot] [M_2] \quad (35)$$

In order to find the rate at which the two monomers enter into the copolymer, equation 34 is divided by equation 35 to give the copolymer composition equation:

$$\frac{d[M_1]}{d[M_2]} = \frac{k_{11} [M_1 \cdot] [M_1] + k_{21} [M_2 \cdot] [M_1]}{k_{12} [M_1 \cdot] [M_2] + k_{22} [M_2 \cdot] [M_2]} \quad (36)$$

The low concentrations (e.g. 10^{-8} moles/liter) of the radical chains in the systems are very hard to experimentally determine. So, to remove these from the equation, the steady state approximation is normally employed. Therefore, a steady state concentration is assumed for both of the species $M_1 \cdot$ and $M_2 \cdot$ separately. The interconversion between the two species must be equal in order for the concentrations of each to remain constant and hence the rates of reactions 31 and 32 must be equal:

$$k_{21} [M_2 \cdot] [M_1] = k_{12} [M_1 \cdot] [M_2] \quad (37)$$

Rearrangement of equation 37 and combination with equation 36 gives:

$$\frac{d[M_1]}{d[M_2]} = \frac{\frac{k_{11} k_{21} [M_2 \cdot] [M_1]^2}{k_{12} [M_2]} + k_{21} [M_2 \cdot] [M_1]}{k_{22} [M_2 \cdot] [M_2] + k_{21} [M_2 \cdot] [M_1]} \quad (38)$$

This equation can be further simplified by dividing the right side and the top and bottom by $k_{21} [M_2 \cdot] [M_1]$. The results are then combined with the parameters r_1 and r_2 , which are defined to be the reactivity ratios:

$$r_1 = \frac{k_{11}}{k_{12}} \quad \text{and} \quad r_2 = \frac{k_{22}}{k_{21}} \quad (39)$$

The most familiar form of the copolymerization composition equation is then obtained as:

$$\frac{d[M_1]}{d[M_2]} = \frac{[M_1] (r_1 [M_1] + [M_2])}{[M_2] ([M_1] + r_2 [M_2])} \quad (40)$$

The ratio of the rates of addition of each monomer can also be considered to be the ratio of the molar concentrations of the two monomers incorporated in the copolymer, which is denoted by (m_1/m_2) . The copolymer composition equation can then be written as:

$$\frac{m_1}{m_2} = \frac{[M_1] (r_1 [M_1] + [M_2])}{[M_2] ([M_1] + r_2 [M_2])} \quad (41)$$

The copolymer composition equation defines the molar ratios of the two monomers that are incorporated into the copolymer, $d[M_1] / d[M_2]$. As seen in the equation, this term is directly related to the concentration of the monomers that were in the feed, $[M_1]$ and $[M_2]$, and also the monomer reactivity ratios, r_1 and r_2 . The ratio of the rate constant for the addition of its own type of monomer to the rate constant for the addition of the other type of monomer is defined as the monomer reactivity ratio for each monomer in the system. When $\wedge\wedge\wedge M_1 \cdot$ prefers to add the monomer M_1 instead of monomer M_2 , the r_1 value is greater than one. When $\wedge\wedge\wedge M_1 \cdot$ prefers to add monomer M_2 instead of monomer M_1 , the r_1 value is less than one. When the r_1 value is equal to zero, the monomer M_1 is not capable of adding to itself, which means that homopolymerization is not possible.

The copolymer composition equation can also be expressed in mole fractions instead of concentrations, which helps to make the equation more useful for experimental studies. In order to put the equation into these terms, F_1 and F_2 are the mole fractions of M_1 and M_2 in the copolymer, and f_1 and f_2 are the mole fractions of monomers M_1 and M_2 in the feed. Therefore:

$$f_1 = 1 - f_2 = \frac{[M_1]}{[M_1] + [M_2]} \quad (42)$$

and:

$$F_1 = 1 - F_2 = \frac{d[M_1]}{d[M_1] + d[M_2]} \quad (43)$$

Then, combining equations 42, 43 and 40 gives:

$$F_1 = \frac{r_1 f_1^2 + f_1 f_2}{r_1 f_1^2 + 2 f_1 f_2 + r_2 f_2^2} \quad (44)$$

This form of the copolymer equation gives the mole fraction of monomer M_1 introduced into the copolymer.²⁷

Different types of monomers show different types of copolymerization behavior. Depending on the reactivity ratios of the monomers, the copolymer can incorporate the comonomers in different ways. The three main types of behavior that copolymerizations tend to follow correspond to the conditions where r_1 and r_2 are both equal to one, when $r_1 \cdot r_2 < 1$ and when $r_1 \cdot r_2 > 1$.

A perfectly random copolymerization is achieved when the r_1 and r_2 values are both equal to one. This type of copolymerization will occur when the two different types of propagating species, $\text{M}_1\cdot$ and $\text{M}_2\cdot$, show the exact same preference for the addition of each type of monomer. In other words, the growing radical chains do not prefer to add one of the monomers more than the other monomer, which results in perfectly random incorporation into the copolymer.

An alternating copolymerization is defined as $r_1 = r_2 = 0$. The polymer product in this type of copolymerization shows a non-random equimolar amount of each comonomer that is incorporated into the copolymer. This may occur because the growing radical chains will not add to its own monomer. Therefore, the opposite monomer will have to be added to produce a growing chain and a perfectly alternating chain.

When $r_1 > 1$ and $r_2 > 1$, both of the monomers want to add to themselves and in theory could produce block copolymers. But in actuality, because of the short lifetime of

the propagating radical, the product of such copolymerizations produce very undesirable heterogeneous products that include homopolymers. Therefore, macroscopic phase separation could occur and desirable physical properties such as transparency would not be achieved.

DETERMINATION OF REACTIVITY RATIOS

Many methods have been used to estimate reactivity ratios of a large number of comonomers.³⁵ The copolymer composition may not be independent of conversion. This means the disappearance of monomer one may be faster than the disappearance of monomer two, if monomer one is being incorporated into the copolymer at a faster rate and therefore it has a larger reactivity ratio than monomer two.

The approximation method² is the simplest of the methods that has been used to calculate the reactivity ratios of copolymer systems. The method is based on the fact that r_1 , the reactivity ratio of component one, is mainly dependent on the composition of monomer two, m_2 , that has been incorporated into the copolymer, at low concentrations of monomer two in the feed, M_2 . The expression is thus:

$$r_1 = M_2 / m_2 \quad (45)$$

The value of the reactivity ratio for component one can be easily determined by only one experiment, but the value is only an approximation and does not provide any validity of the estimated r_1 . In order to determine the amount of the comonomer that has been incorporated into the copolymer, various analytical methods must be used. Proton Nuclear Magnetic Resonance, Carbon 13 NMR and Fourier Transform Infrared

Spectroscopy are three sensitive instruments that can determine the copolymer composition. The approximation method is limited when the reactivity ratio of one of the components in the system has a value of less than 0.1 or greater than a value of 10. However, the method does give good insight into the reactivity ratio values for many copolymer systems. The approximation of reactivity ratios can be easy and quick when using this method of evaluation.

The Mayo-Lewis intersection method^{32,36} uses a linear form of the copolymerization equation where r_1 and r_2 are linearly related:

$$r_1 = r_2 (m_1 M_2^2 / m_2 M_1^2) + (M_2 / M_1)[(m_1 / m_2) - 1] \quad (46)$$

By using the equations $m_1 M_2^2 / m_2 M_1^2$ and $(M_2 / M_1)[(m_1 / m_2) - 1]$ for the slope and intercept respectively, a plot can be produced for a set of experiments, after the copolymer composition has been determined. The straight lines that are produced on the plot for each experiment, where r_1 represents the ordinate and r_2 represents the abscissa, intersect at a point on the r_1 vs. r_2 plot. The point where these lines meet is taken to be r_1 and r_2 for the system in study. The main advantage of this method is that it gives a qualitative observation of the validity of the intersection area. Over the whole range of possible copolymer compositions that were tested, more compact intersections, better define the data. However, the method requires a visual check of the data and a quantitative estimation of the error is impossible. Therefore, weighting of the data is needed to determine the most precise values of r_1 and r_2 .

The Fineman-Ross linearization method³⁷ uses another form of the copolymer equation:

$$G = r_1 H - r_2 \quad (47)$$

Where $G = m_1/m_2 (1 - (M_2/M_1)) \quad (48)$

And $H = (m_1/m_2)^2 (M_2/M_1) \quad (49)$

For this method, by plotting G versus H for all the experiments, one will obtain a straight line where the slope of the straight line is the value for r_1 and the intercept of the line is the value for r_2 . This type of reactivity ratio determination has the same advantages and disadvantages of the method described above, however, this treatment is a linear least squares analysis instead of a graphical analysis. The validity is only qualitative and the estimates of r_1 and r_2 can change with each experimenter by weighting the data in different ways. Furthermore, the high and low experimental composition data are unequally weighted, which produces large effects on the calculated values of r_1 and r_2 . Therefore, different values of r_1 and r_2 can be produced depending on which monomer is chosen as M_1 .²⁷

A refinement of the linearization method was introduced by Kelen and Tudos³⁸⁻⁴⁰ by adding an arbitrary positive constant α into the Fineman and Ross equation 47. This technique spreads the data more evenly over the entire composition range to produce equal weighting to all the data.²⁷ The Kelen and Tudos refined form of the copolymer equation is as follows:

$$\eta = [r_1 + r_2/\alpha] \xi - r_2/\alpha \quad (50)$$

where:

$$\eta = G/(\alpha + H) \quad (51)$$

$$\xi = H/(\alpha + H) \quad (52)$$

By plotting η versus ξ , a straight line is produced that gives $-r_2/\alpha$ and r_1 as the intercepts on extrapolation to $\xi=0$ and $\xi=1$, respectively. Distribution of the experimental data symmetrically on the plot is performed by choosing the α value to be $(H_m H_M)^{1/2}$ where H_m and H_M are the lowest and highest H values, respectively. Even with this more complicated monomer reactivity ratio technique, statistical limitations are inherent in these linearization methods.^{41,42} O'Driscoll, Reilly et al^{43,44} determined that the dependent variable does not truly have a constant variance and the independent variable in any form of the linear copolymer equation is not truly independent. Therefore, analyzing the composition data using a non-linear method has come to be the most statistically sound technique.

The non-linear or curve-fitting method³¹ is based on the copolymer composition equation in the form:

$$m_1/m_2 = (r_1 M_1^2 + M_1 M_2) / (r_2 M_2^2 + M_1 M_2) \quad (53)$$

This equation is based on the assumptions that the monomer concentrations do not change much throughout the reaction and the molecular weight of the resulting polymer is relatively high. In order to determine reactivity ratios from the experimental data, a graph must be generated for the observed comonomer amount that was incorporated into the copolymer, m_1 , versus the feed comonomer amount, M_1 , for the entire range of comonomer concentrations. Then a curve can be drawn through the points for selected r_1 and r_2 values and the validity of the chosen reactivity ratio values can be checked by changing the r_1 and r_2 values until the experimenter can demonstrate that the curve best fits the data points.

The main advantage of the reactivity ratio determination methods discussed thus far is the results can be visually and qualitatively checked. Disadvantages include, a direct dependence of the composition on conversion for most polymer systems and, therefore, low conversion (e.g. instantaneous composition) is needed to determine the reactivity ratios. Furthermore, extensive calculations are required, but only qualitative measurements of precision can be obtained. Finally, weighting of the experimental data for the methods to determine precise reactivity ratios is hard to reproduce from one experimenter to another.

Therefore, a technique that allows the rigorous application of statistical analysis for r_1 and r_2 was proposed by Mortimer and Tidwell, which they called the nonlinear least squares method.^{2,45-48} This method can be considered to be a modification or extension of the curve fitting method. For selected values of r_1 and r_2 , the sum of the squares of the differences between the observed and the computed polymer compositions is minimized. Using this criterion for the nonlinear least squares method of analysis, the values for the reactivity ratios are unique for a given set of data, where all investigators arrive at the same values for r_1 and r_2 by following the calculations. Recently, a computer program published by van Herck^{3,4} allows, for the first time, rapid data analysis of the nonlinear calculations. It also permits the calculations of the validity of the reactivity ratios in a quantitative fashion.⁴⁹ The computer program produces reactivity ratios for the monomers in the system with a 95% joint confidence limit determination. The joint confidence limit is a quantitative estimation of the validity of the results of the experiments and the calculations performed. This method of data analysis consists of obtaining initial estimates of the reactivity ratios for the system and experimental data of

comonomer charge amounts and comonomer amounts that have been incorporated into the copolymer, both in mole fractions. Many repeated sets of calculations are performed by the computer, which rapidly determines a pair of reactivity ratios that fit the criterion, wherein the value of the sum of the squares of the differences between the observed polymer composition and the computed polymer composition is minimized.^{50,51} This method uses a form of the copolymer composition equation with mole fractions of the feed. It amounts to determining the mole fraction of the comonomer that should be incorporated into the copolymer during a differential time interval.

$$F_2 = \frac{r_2 f_2^2 + f_2 f_1}{r_2 f_2^2 + 2f_1 f_2 + r_1 f_1^2} \quad (54)$$

For this equation, F_2 represents the mole fraction of comonomer two that was calculated to be incorporated into the copolymer and f_1 and f_2 represent the mole fractions of each comonomer that were fed into the reaction mixture. The use of the Gauss-Newton nonlinear least squares procedure predicts the reactivity ratios for a given set of data after repeating the calculations so that the difference between the experimental data points and the calculated data points on a plot of mole fraction of comonomer incorporated versus comonomer in the feed is reduced to the minimum value.^{52,53} Therefore, the last iteration of the calculations produces a convergence on the least squares estimate of r_1 and r_2 .⁵⁴

The estimate of errors for this type of calculation is dependent on the assumption that the random errors inherent in the experimentally determined values for the comonomer fraction incorporated into the copolymer are evenly distributed throughout the experimental data. Therefore, it would follow that the differences in the values for

the comonomer fractions in the copolymer during the time intervals are evenly distributed with constant variances and will produce a method for determining joint confidence limits. The 95% joint confidence limits determine the values where the reactivity ratios can lie with a 95% probability. On a plot of the reactivity ratio of monomer one versus the reactivity ratio of monomer two, the joint confidence limits are, in general, elliptical figures due to the nonlinear calculations that were performed.²

Chapter III. Experimental

CHEMICALS, PURIFICATION AND REACTION APPARATUS

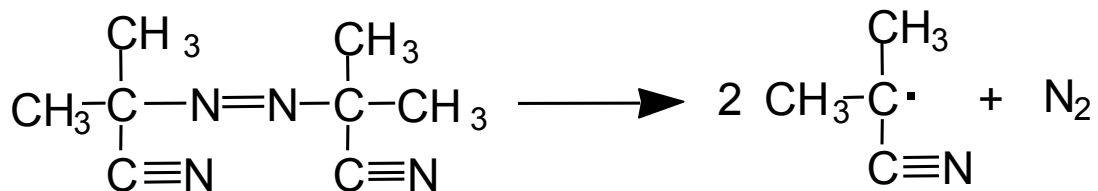
Homo- and copolymerization experiments were performed in a fume hood with a clean, generally 250 ml three neck round bottom flask. A submerged nitrogen needle purge was fitted to the flask and nitrogen purging was conducted for 20 minutes prior to the reaction in order to remove all oxygen. The solution of monomers and solvent was purged after addition to the flask for at least 20 minutes prior to heating and then purged throughout the reaction. A thermocouple was also fitted to the reaction vessel to monitor the temperature of the reaction so that the hot plate stirrer could maintain the light mineral oil bath and, thus, the reaction vessel at the correct temperature. The thermocouple regulated the temperature at a constant 62°C throughout the reaction. A condenser was used on one of the necks of the flask in order to condense any monomers

that might otherwise possibly escape. A magnetic bar was used to stir the solution at a constant speed in order to assure even distribution of monomer and initiator concentrations throughout the entire volume of solution. A rubber septum was used to cover one of the three necks. This septum was removed to add monomers and solvents, and when the temperature reached 62° C the initiator was added through the neck. Then the septum was replaced onto the flask and the reaction was allowed to proceed.

The flask was immersed in a light mineral oil bath that contained a magnetic stir bar and a thermocouple. The thermocouple was used to regulate the temperature of the oil bath. The stir bars in the oil bath and in the reaction vessel were regulated by the stirrer hot plate that was below the oil bath and on top of an adjustable jack stand. The adjustable jack stand was used to raise and lower the oil bath so that the reaction vessel could be heated or cooled in an easy fashion. Two adjustable arm clamps were used, one to hold the reaction kettle and the other to support the condenser.

The organic solvent was N, N-dimethylformamide, DMF (Aldrich). It was purified by distillation with calcium hydride (CaH_2) to remove impurities, including water. N, N-dimethylformamide has a molecular weight of 73.09 grams per mole, density of 0.944 grams per milliliter and a molecular formula of $\text{HCON}(\text{CH}_3)_2$. Acrylonitrile, AN, (Aldrich) was purified by passing through an activated alumina column to remove impurities such as inhibitors. The presence of 45 parts per million of monomethyl ether hydroquinone in the monomer from Aldrich is intended to inhibit the polymerization during transport and storage by scavenging the free radicals. After the inhibitor was removed from the monomer, the purified monomer was refrigerated so that the monomers do not undergo degradation or premature polymerization. The molecular

weight of acrylonitrile is 54.06 grams per mole and the molecular formula is $\text{H}_2\text{C}=\text{CHCN}$. It is a clear liquid that has a boiling point of 77°C and a density of 0.806 grams per milliliter. Since this material is a known cancer-causing agent, extreme caution must be taken when handling and disposing of it in order to reduce the risk of contact and ground water contamination. Methyl acrylate, MA, was obtained from Aldrich and the inhibitors and impurities were removed by passing the monomer through an activated alumina column. The methyl acrylate contained 100 parts per million of monomethyl ether hydroquinone as the inhibitor. The purified monomer must also be refrigerated and stored in a sealed container. The molecular weight of this monomer is 86.09 grams per mole with a molecular formula of $\text{H}_2\text{C}=\text{CHCO}_2\text{CH}_3$. This is a clear liquid that has a boiling point of 80°C and a density of 0.956 grams per milliliter. The free radical initiator that was used for all the experiments was 2,2'-azobisisobutyronitrile, AIBN, which was also obtained from Aldrich Chemicals. Its molecular weight is 164.21 grams per mole and the molecular formula is $(\text{CH}_3)_2\text{C}(\text{CN})\text{N}=\text{NC}(\text{CH}_3)_2\text{CN}$. AIBN is a white powder with a melting point of 104°C . The thermal decomposition of AIBN occurs at lower temperatures and produces a maximum of two free radicals and a nitrogen side product as shown in Figure 6.



AIBN

Figure 6: Thermal decomposition of AIBN to form two radicals and nitrogen

COPOLYMERIZATION

The reaction scheme for the copolymerization of acrylonitrile and methyl acrylate in N,N-dimethylformamide using AIBN as the free radical initiator at 62°C is shown in Figure 7.

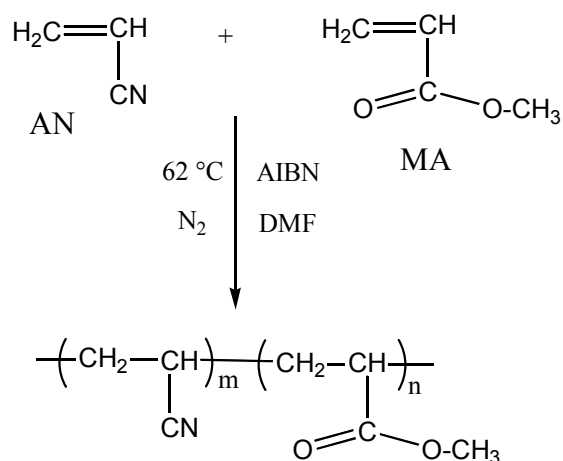


Figure 7: Reaction Scheme for the Copolymerization of Acrylonitrile and Methyl Acrylate

This thesis research was limited to batch reactions, where all the reactants were charged at the beginning of the reaction.⁵⁵ The reaction began with the initial heating of the oil bath to 62°C with stirring of the reaction components in the flask while purging with nitrogen for twenty minutes. The purified monomers and all but 10 ml of solvent were added into a clean three neck round bottom flask that was fitted with a condenser, thermocouple, nitrogen purge and magnetic stir bar. Nitrogen was

purged through the solution system for twenty minutes prior to heating. The solution was then heated to 62°C by raising the oil bath so that the oil covered up the volume of solution in the vessel. The initiator was dissolved in 5 ml of solvent (0.3 mol/liter) and was then added to the monomer solution to start the polymerization at 62°C. The AIBN container was rinsed with the remaining 5 ml of DMF and this solution was then added to the reaction flask. Various amounts of acrylonitrile and methyl acrylate were used to change the charging ratios in a systematic manner, but the total monomer weight was kept constant at 20% solids. The amount of DMF also varied, but the weight percent relative to the monomers remained constant at 80%. Furthermore, the amount of AIBN that was added to the reactions was held constant at a half mole percent relative to the monomers. Table 3 indicates the amounts of each monomer and the amount of the solvent and initiator that were added to the reaction flask to produce a methodical study of the copolymer composition. The entire range of data provided for a systematic study, with 5% intervals, of the copolymerization of acrylonitrile and methyl acrylate over a range of 90/10 to 10/90 of AN/MA monomer mole percent feed ratios.

For this study, copolymerization times were varied in order to obtain less than 10% monomer conversion. The reaction was quenched by placing the flask in an ice bath, which cooled the reaction to temperatures that essentially stopped the decomposition of the AIBN initiator.

AN Ratio	MA Ratio	AN (g)	MA (g)	AN(mol)	MA (mol)	AIBN (mol)	AIBN (g)	Total monomer wt	DMF (ml)
90	10	17.00	3.065	0.320	0.0356	0.00178	0.292	20.06	80.32
85	15	16.00	4.582	0.301	0.0532	0.00177	0.291	20.58	82.31
80	20	14.30	5.801	0.269	0.0673	0.00168	0.276	20.10	80.41
75	25	13.00	7.031	0.245	0.0816	0.00163	0.268	20.03	80.13
70	30	11.9	8.275	0.224	0.0961	0.00160	0.263	20.17	80.7
65	35	11.00	9.611	0.207	0.111	0.00159	0.261	20.61	82.45
60	40	9.7	10.49	0.182	0.121	0.00152	0.250	20.19	80.77
55	45	8.7	11.54	0.163	0.134	0.00149	0.244	20.24	80.99
50	50	7.80	12.65	0.147	0.147	0.00147	0.241	20.45	81.83
45	55	6.7	13.28	0.126	0.154	0.00140	0.230	19.98	79.95
40	60	5.9	14.35	0.111	0.166	0.00139	0.228	20.25	81.04
35	65	5.00	15.06	0.094	0.175	0.00134	0.221	20.07	80.28
30	70	4.2	15.90	0.0791	0.184	0.00132	0.216	20.10	80.4
25	75	3.5	17.03	0.0659	0.197	0.00131	0.216	20.53	82.15
20	80	2.70	17.53	0.050	0.203	0.00127	0.208	20.23	80.92
15	85	2	18.38	0.0376	0.213	0.00125	0.206	20.38	81.55
10	90	1.30	18.99	0.024	0.220	0.00122	0.201	20.29	81.2

Table 3: Calculations of amounts of comonomers, initiator and solvent employed in the copolymerization study

ISOLATION OF THE COPOLYMER

The copolymer was precipitated in an excess of water in order to determine the percent conversion. Extremely careful techniques were used so as to minimize the loss of any solution, or precipitate during the isolation process. A 1200 ml blender was used to stir the water while the copolymer solution was added drop-wise to the agitated water.

About 10 ml of solution was added to 800 ml of water and the process was repeated, until

no solution was left in the flask. The copolymer was filtered from the water solution by vacuum filtration using a Buchner funnel with a house vacuum (about 10 mm). The water-monomer solution was discarded in a labeled waste container so that no contamination, e.g. of the ground water, could occur. The filter paper that was used in the Buchner funnel was pre-weighed so that the copolymer percent yield was as accurate as possible. The polymer cake was washed two times with 250 ml of methanol. The methanol removed the excess monomer that could still be present in the copolymer filter cake and also removed the water so the copolymer cake could be dried much easier. The methanol was discarded into the proper container and the filter cake was allowed to air dry by keeping the vacuum on and allowing air to pass through the white copolymer filter cake for a period of ten minutes.

Further drying of the copolymer was performed in a vacuum oven at elevated temperatures (up to 70° C). The copolymer and the filter paper were placed in a large crystallizing dish and then put into a vacuum oven. The temperature of the vacuum oven was increased slowly in order for the water and methanol to diffuse out of the copolymer. The temperature of the vacuum oven was increased to a maximum of 70° C and the polymer and filter were left in the oven for a minimum of 8 hours. After that time, the copolymer and paper filter were removed from the oven and allowed to cool to room temperature. The copolymer and the filter were then weighed and the weight of the paper filter was subtracted from the total weight of the copolymer and filter. Thus, the weight of the copolymer was determined. Calculations were then performed in order to determine the percent conversion of the monomers. All the copolymers that were used in the study were produced during the first 10% monomer conversion and the copolymers

that were produced that had a higher value than 10% conversion were set aside and not used in the current study on reactivity ratios.

PROTON NUCLEAR MAGNETIC RESONANCE

In order to determine the amount of each comonomer that was incorporated into the copolymer, proton nuclear magnetic resonance, ^1H NMR, was performed on each copolymer. This type of analytical technique used to determine the amounts of each structure in a copolymer is widely accepted and used both in the industry and academia at the present time for the study of polymerization kinetics.⁵⁶⁻⁵⁸

All of the ^1H NMR samples were dissolved in deuterated-dimethyl sulfoxide, d_6 -DMSO, and placed into a warm water ultrasonic bath. An ultrasonic bath was used to quickly dissolve the copolymers that afforded the required copolymer solutions. ^1H NMR experiments produced well-resolved peaks that corresponded to the methyl group on the methyl acrylate structure and the methylene groups on both the acrylonitrile and methyl acrylate comonomers that were incorporated into the copolymer. Figure 8 shows the ^1H NMR spectrum of an 85/15 AN/MA copolymer and the assigned peaks that were used in the calculations to determine the amount of each comonomer.

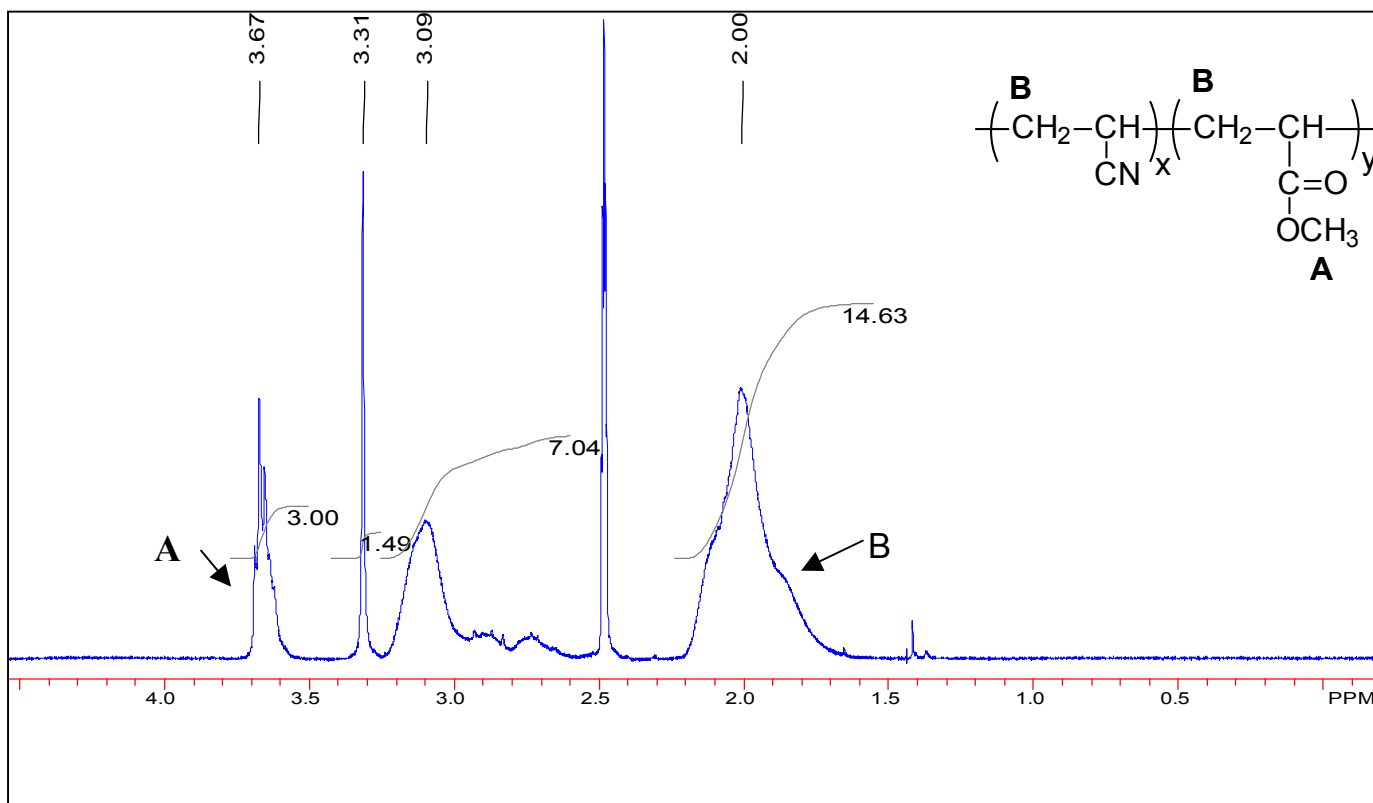
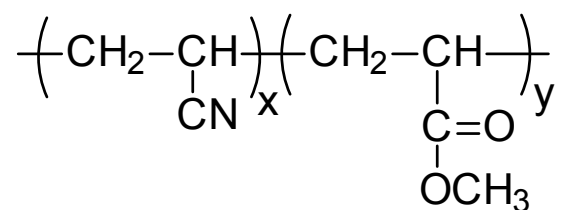


Figure 8: ^1H NMR of Acrylonitrile and Methyl Acrylate Comonomer Peaks in a 85/15 copolymer: A and B Peaks Correspond to the Methyl and Methylene Groups

The integrals of the methyl peak and the methylene peak were used for the calculations to determine the amount of each comonomer that was incorporated into the precipitated copolymer. If x and y represent how many acrylonitrile and methyl acrylate monomer structures were incorporated into the copolymer and the observed values of the integrals for the methyl and methylene peaks are n and m respectively, then the calculations to determine the amount of each monomer incorporated are as follows:



Three methyl protons give: $3y = n$

$$\text{Solve for } y: y = n / 3$$

Two methylene protons from each structure give: $2x + 2y = m$

$$\text{Substitute for } y \text{ and solve for } x: 2x + 2n / 3 = m$$

$$2x = m - 2n / 3$$

$$x = 1 / 2 (m - 2n / 3)$$

Utilize the values for the integrals of each peak into the x and y equations and use the following equation to obtain the percent of methyl acrylate that was incorporated into the copolymer:

$$\% \text{ MA} = \frac{y}{x + y} * 100$$

In order to obtain the percent of acrylonitrile that was incorporated into the copolymer, the value of the percent methyl acrylate was subtracted from a value of 100%:

$$\% \text{ AN} = 100\% - \% \text{ MA}$$

By using these calculations for each experiment performed, the amount of each comonomer incorporated was determined for the samples that were precipitated after the copolymerization was allowed to proceed for no more than 10 % monomer conversion.

Seventeen different mole percent charge ratios were performed as shown in Table 3. The copolymers for these different charge ratios were precipitated in an excess of water and washed with methanol to remove any remaining monomers, which could alter the experimental results. The isolated copolymers were then dried and weighed. After the weighing of the copolymers, a sample was removed and dissolved in d_6 -DMSO for the ^1H NMR experiments. A JEOL USA 500 MHz NMR instrument was used in the single pulse mode to obtain the spectra at room temperature for all the precipitated copolymers. The use of this extremely high field instrument helped to resolve the methyl and methylene peaks of the copolymer. Previous studies in the literature to determine the copolymer compositions produced relatively poor ^1H NMR spectra that contained overlapped peaks of the methyl and methylene peaks with other peaks in the spectra. Therefore, precise determination of the copolymer compositions was difficult. The use of this 500 MHz magnetic field allowed one to resolve the peaks and produce a spectrum of value. For each mole percent charge ratio that was conducted, ^1H NMR produced the corresponding mole percent values of each comonomer incorporated into the copolymer.

MOLECULAR WEIGHT DETERMINATION

Gel permeation chromatography, GPC (often referred to as Size Exclusion Chromatography [SEC]), was conducted on selected samples to determine the molecular weight of the copolymers that were produced. A Waters 150C ALC/GPC chromatograph was used at 60° C. A weight of 0.02 grams of the copolymer was dissolved in 1-methyl-2-pyrrolidinone, NMP, and 0.02 molar phosphorus pentoxide, P₂O₅. The flow of the mobile phase (NMP with 0.02M P₂O₅) through the column was 1ml/min and the column used was a Waters StyragelHRO.5+2+3. The flow of the mobile phase through the column contained the copolymer and the packing in the column contains different porosities that fractionate the copolymer molecules. The elution time is a relative measure of the size and allows calculation of molecular weights of the copolymer via hydrodynamic calibrations. Two detectors (a refractive index detector and a Viscotek Mode 100 viscosity detector) were used in parallel to detect the copolymers as they eluted from the separation column. Figure 9 shows the GPC chromatogram for a 15/85 mole percent AN/MA sample in NMP + 0.02M P₂O₅ at 60° C.

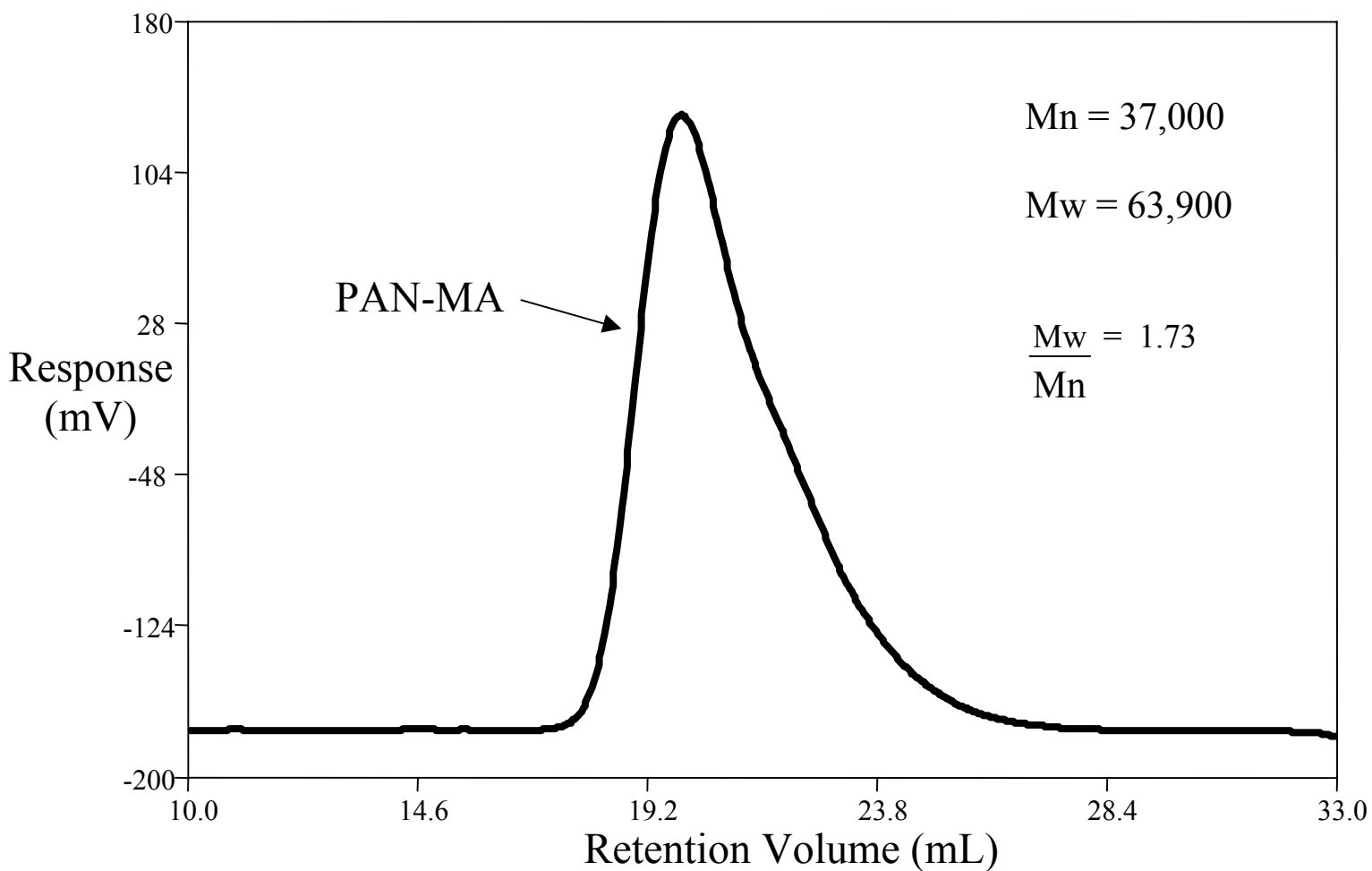


Figure 9: Raw GPC chromatogram of a 15/85 mole % AN/MA copolymer in NMP + 0.02M P_2O_5 at 60°C (from differential refractometric detector)

Figure 9 shows the apparent molecular weight distribution peak is monomodal. The number average molecular weight of this copolymer (\bar{M}_n) was determined via universal calibration⁵⁹ to be 37,000 grams per mole, which indicates a high molecular weight, comparable to other carbon fiber precursor materials. High molecular weight

was also advantageous since loss of copolymer during the precipitation and filtering processes might occur if low molecular weight copolymers were produced.

REAL TIME INFRARED SPECTROSCOPY

Many different methods have been used by polymer scientists to monitor the real time dependence of the disappearance of the mole fractions of the comonomers and the production of the copolymers during free radical copolymerizations.⁶⁰ Unfortunately the success of other forms of monitoring has often been limited. The traditional method of determining the copolymerization kinetics is where many experiments are conducted over a wide range of monomer feed ratios and allowed to copolymerize to low conversion. Then, the copolymer is precipitated into an excess amount of non-solvent and dried under vacuum. Typically the copolymer is weighed and the percent conversion is determined by simple calculations. Then a sample is dissolved in a deuterated solvent and NMR experiments (or alternatively elemental analyses) are conducted on the sample to determine how much of each monomer was incorporated into the copolymer. This is a time consuming and, therefore, expensive way to determine copolymerization kinetics. The use of real time-IR as an analytical tool to determine the copolymer composition could be applied to certain systems that show well resolved peaks for the monomers in solution so as to monitor the disappearance of the area under the peaks. All the kinetic data can then be more efficiently and accurately obtained relative to the traditional approach.

The use of *in situ* Fourier Transfer Infrared Spectroscopy, FTIR, is a relatively new development to study polymerization. The instrument principles and capabilities of the ReactIR 1000 that was based on attenuated total reflectance (ATR) have been described in detail previously.⁶¹ The real time *in situ* FTIR yields a large amount of differential copolymerization data from only a few experiments. A large amount of data is required to derive more precise values for the reactivity ratios of the copolymerization system. The infrared spectrometer can monitor the disappearance of the appropriate well-resolved comonomer peaks as the polymerization process proceeds. The disappearance of the comonomers is directly related to the production of the copolymer. A major advantage of this type of *in situ* study is that the copolymers do not need to be isolated or precipitated. Since the copolymer composition is directly related to the comonomer peak area loss, the copolymer composition was determined directly in solution. Therefore, the time consuming process of precipitation and drying of the material is not needed. This makes the process of determining copolymer composition very easy, quick and accurate.

As discussed in the previous chapter, the use of the copolymer composition equation for the disappearance of the comonomers can be used:

$$\frac{d[M_1]}{d[M_2]} = \frac{[M_1] (r_1[M_1] + [M_2])}{[M_2] ([M_1] + r_2[M_2])} \quad (54)$$

The ratio of the rates of addition of each monomer is also the ratio of the molar concentrations of the two monomers in the copolymer, which is denoted by (m_1/m_2) . The copolymer composition equation can then be written as:

$$\frac{m_1}{m_2} = \frac{[M_1] (r_1 [M_1] + [M_2])}{[M_2] ([M_1] + r_2 [M_2])} \quad (55)$$

The copolymer composition equation determines the molar ratios of the two monomers that are incorporated into the copolymer, $d[M_1]/d[M_2]$. The equation shows this term is directly related to the concentration of the monomers that were in the feed, $[M_1]$ and $[M_2]$, and also the monomer reactivity ratios, r_1 and r_2 . The ratio of the rate constant for the addition of its own type of monomer to the rate constant for the addition of the other type of monomer is the monomer reactivity ratio for each monomer in the system.

The copolymer composition equation can also be expressed in mole fractions instead of concentrations, which helps to make the equation more useful for experimental purposes. In order to put the equation into these terms, F_1 and F_2 are the mole fractions of M_1 and M_2 in the copolymer, and f_1 and f_2 are the mole fractions of monomers M_1 and M_2 in the feed. Therefore:

$$f_1 = 1 - f_2 = \frac{[M_1]}{[M_1] + [M_2]} \quad (56)$$

and:

$$F_1 = 1 - F_2 = \frac{d[M_1]}{d[M_1] + d[M_2]} \quad (57)$$

Then, combining the copolymer equation and the previous two equations gives:

$$F_1 = \frac{r_1 f_1^2 + f_1 f_2}{r_1 f_1^2 + 2 f_1 f_2 + r_2 f_2^2} \quad (58)$$

This form of the copolymer equation gives the mole fraction of monomer M_1 incorporated into the copolymer, F_1 , and can be used for the calculations of the real time FTIR data.

COPOLYMERIZATION USING REAL TIME MID-FTIR

The experiments were set up in the same fashion as the set up for the batch polymerizations that were isolated, except for the use of the *in situ* FTIR probe. The real time Mid-FTIR, 10,000-4000 cm^{-1} , was conducted *in situ* using an Applied Systems Inc. ReacIR 1000. The probe replaced the rubber septum that was used in one of the necks of the three neck flask that was used in the previous experiments. It was positioned such that the probe was immersed in the solution and still allowed the magnetic stir bar to spin. Careful positioning of the heavy probe was needed so that the neck of round bottom flask was not broken.

The area that was monitored for acrylonitrile was the peak at 690 cm^{-1} and a two-point baseline was used from 680 to 715 cm^{-1} . The two-point base line was used in the calculations of the peak areas as they decreased during the polymerization process. The peak that was monitored for methyl acrylate was at 814 cm^{-1} and the two-point base line that was used in the calculations of the peak area was between 790 and 832 cm^{-1} . Well-

resolved peaks were obtained for the solution of acrylonitrile, methyl acrylate, DMF and AIBN. The infrared spectra of the three compounds DMF, AN and MA are shown in Figure 10.

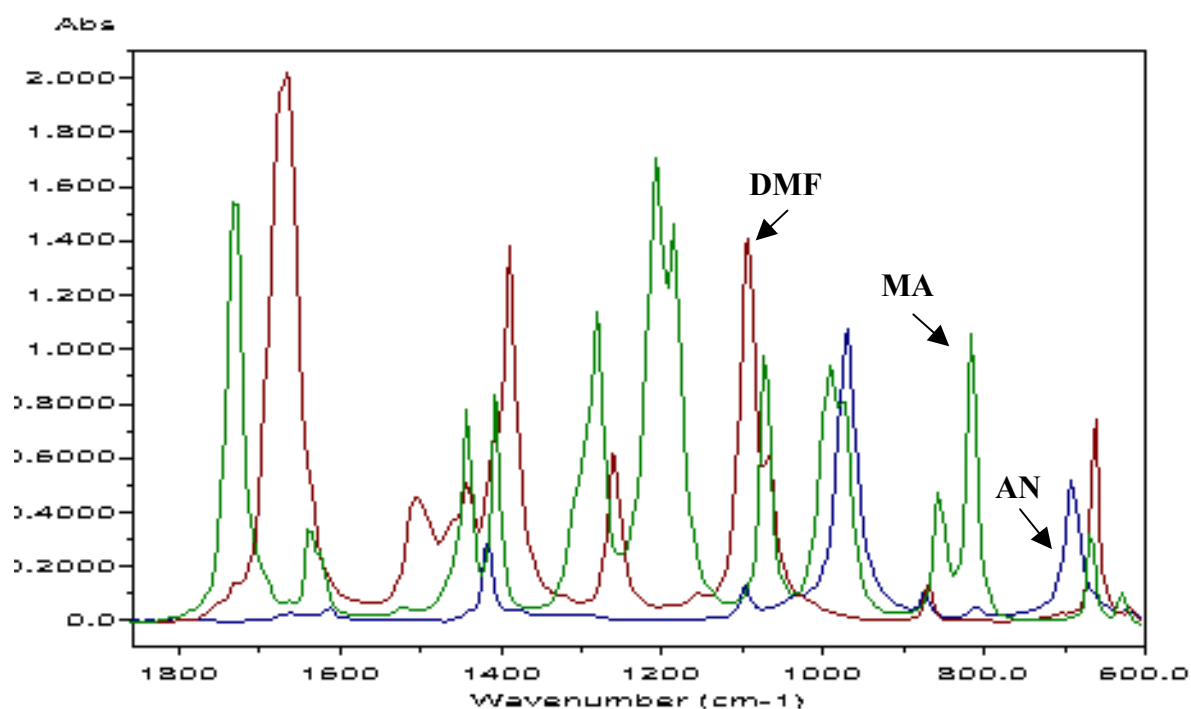


Figure 10: Overlay of AN, MA and DMF infrared peaks as obtained from the insitu FTIR instrument before polymerization

AIBN also did not interfere with the FTIR spectra for this system. Therefore, it was concluded that the IR peaks were resolved well enough for this type of study to be conducted. An enlargement of the two peaks at 690 and 814 cm⁻¹ that were monitored during the copolymerization is shown in Figure 11.

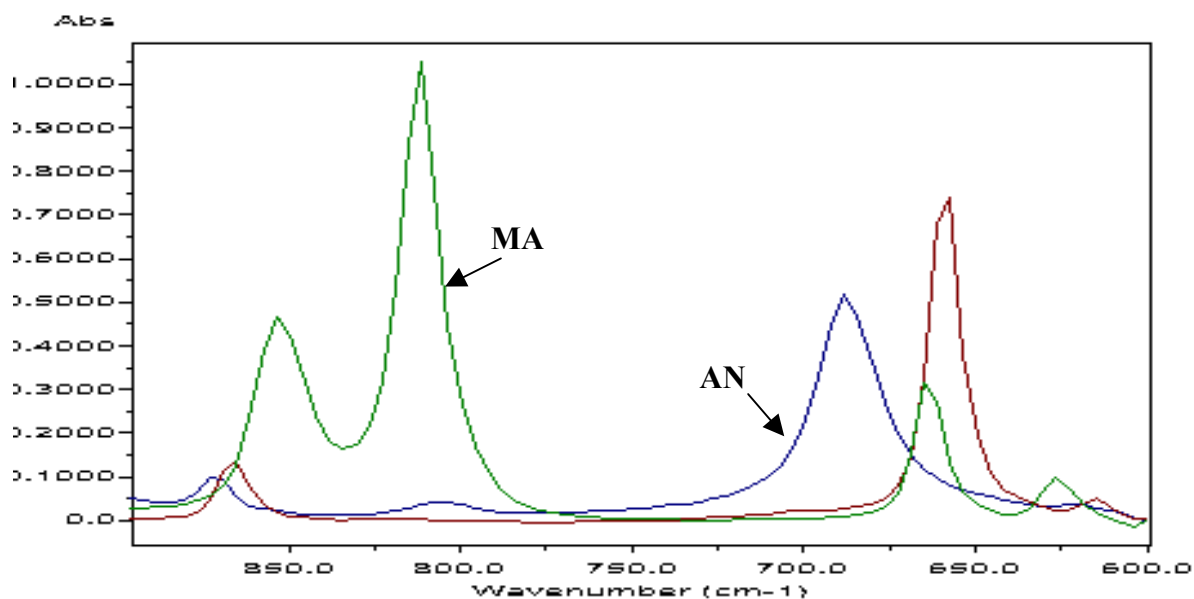


Figure 11: Expansion of the peaks at 690 and 814 cm^{-1} for AN and MA comonomers respectively that were monitored throughout the copolymerization

The copolymerization was begun in the same manner as described above. The spectral data was obtained from just before the AIBN addition until ten percent conversion of the monomers. A data point was taken every 60 seconds for the monomer feed ratios of 90/10, 85/15, 80/20, 65/35, 50/50, 35/65 and 20/80 mole percents of AN/MA. The mole percent feed ratio of 85/15 AN/MA was allowed to polymerize to 80% monomer conversion and the data obtained for the disappearance of the methyl acrylate monomer peak is shown in Figure 12. The real time FTIR monitoring of the methyl acrylate peak conversion can be seen to disappear as the polymerization proceeds;

this is directly related to the incorporation of the methyl acrylate monomer into the copolymer.

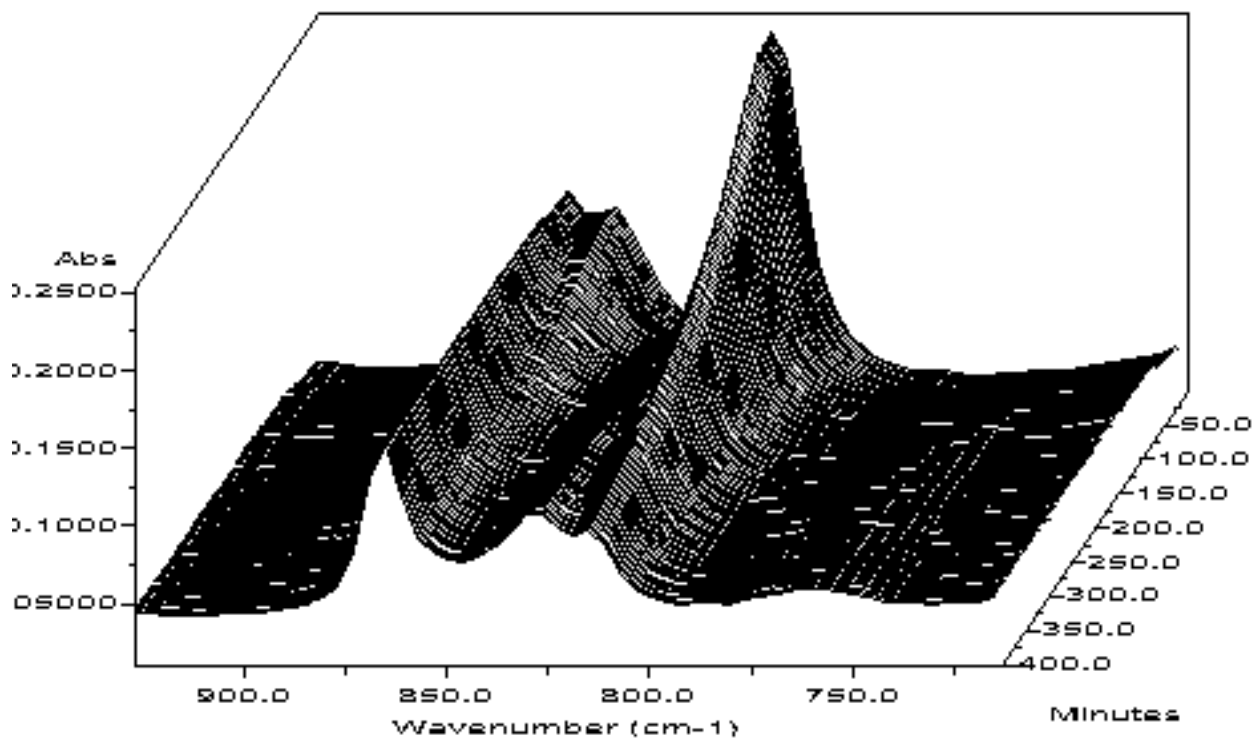


Figure 12: Waterfall plot of the disappearance of the methyl acrylate Monomer peak at 814 cm^{-1} as polymerization proceeds

The AN/MA monomer disappearance for an 85/15 mole percent comonomer feed ratio was well documented with the *in situ* real time FTIR probe. Figure 13 shows the disappearance of the two monomer peaks versus time during polymerization to 80% monomer conversion.

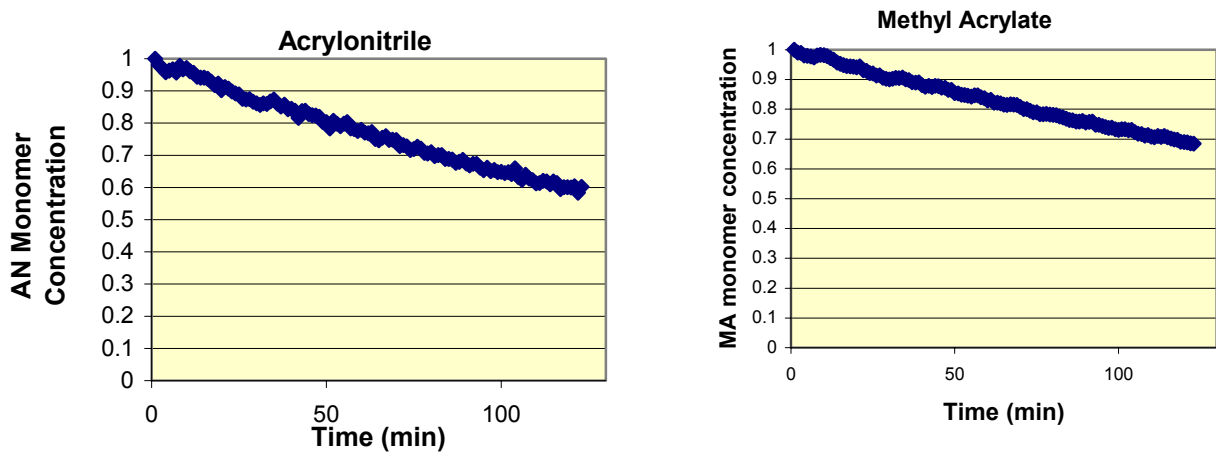


Figure 13: AN/MA monomer disappearance for an 85/15 mole percent feed ratio allowed to polymerize to 80% monomer conversion

Figure 13 shows that as time proceeded throughout the experiment, the monomer peak areas and thus the concentrations decreased. With some advanced calculations, as will be described in the next chapter, the mole fraction of the comonomers that were incorporated into the copolymer can be determined and reactivity ratios for the system of AN and MA can be calculated.

Chapter IV: Results and Discussion

Many different methods have been used to calculate reactivity ratios.^{32,36,37,31} These include the approximation method, intersection method, linearization method and the curve fitting method. The major problem with these methods is that the probable errors can be only qualitatively determined. A visual check of the intersection of lines or the best fit curve can only estimate the amount of error; therefore, only a qualitative determination of error is possible. In order to obtain a quantitative determination of uncertainty, Tidwell and Mortimer² developed a nonlinear least-squares method that was the first technique to allow a rigorous application of statistical analysis for the reactivity ratios r_1 and r_2 . The Mortimer/Tidwell method is an extension of the curve fitting nonlinear model and allows the calculations to be quantitatively analyzed. The nonlinear least-squares method uses selected values of r_1 and r_2 from the literature, or any other type of reactivity ratio determination method, as first approximations and calculates the

sum of the squares of the differences between the observed and the computed copolymer compositions in order for them to be at a minimum. Extensive calculations are needed to determine the minimum sum of the squares of the differences, but a computer program developed by van Herck³ permits rapid analysis of the nonlinear least-squares calculations.

Proton NMR and *in situ* FTIR were used to determine the copolymer compositions. The ¹H NMR experiments needed samples of the copolymer that were isolated and purified so that they could be dissolved in a deuterated solvent where no overlapping peaks were present. The copolymer isolation was a time consuming process and was experimentally difficult. Therefore, the use of the *in situ* FTIR analytical instrument was used. The *in situ* FTIR method permits the monomer conversions to be observed in the DMF solvent by monitoring the infrared absorbance peaks that are associated with each monomer. The time consuming isolation of the copolymers is not needed when using the *in situ* FTIR method, and thus, gives copolymer compositions in a timely and experimentally advantageous fashion.

COPOLYMER COMPOSITION DISTRIBUTION

Throughout the entire range of monomer conversion, the copolymer composition may not be the same for the copolymers produced at the beginning of the reaction and at the end of the reaction. In other words, the copolymer composition may not be independent of conversion. At the beginning of the copolymerization the monomer composition is the same as that charged into the reactor. But, since one of the monomers

has a higher reactivity ratio, it will react more rapidly than the other and the amount of that monomer that is in solution decreases more than the other comonomer. Therefore, the concentration of the monomer with the higher reactivity ratio will be almost zero before the end of the reaction. For example, if the comonomer composition for both monomers in the solution at the beginning of the reaction is 50 mole percent and comonomer 1 has a higher reactivity ratio than comonomer 2, then the disappearance of comonomer 1 will be faster with respect to time than that of comonomer 2. But, in the first 5-10% of comonomer conversion the concentration of each comonomer in solution will not change very much, and therefore, the copolymer composition will reflect the true reactivity of each comonomer in the system. Figure 14 schematically shows the comonomer composition change as the conversion increases.

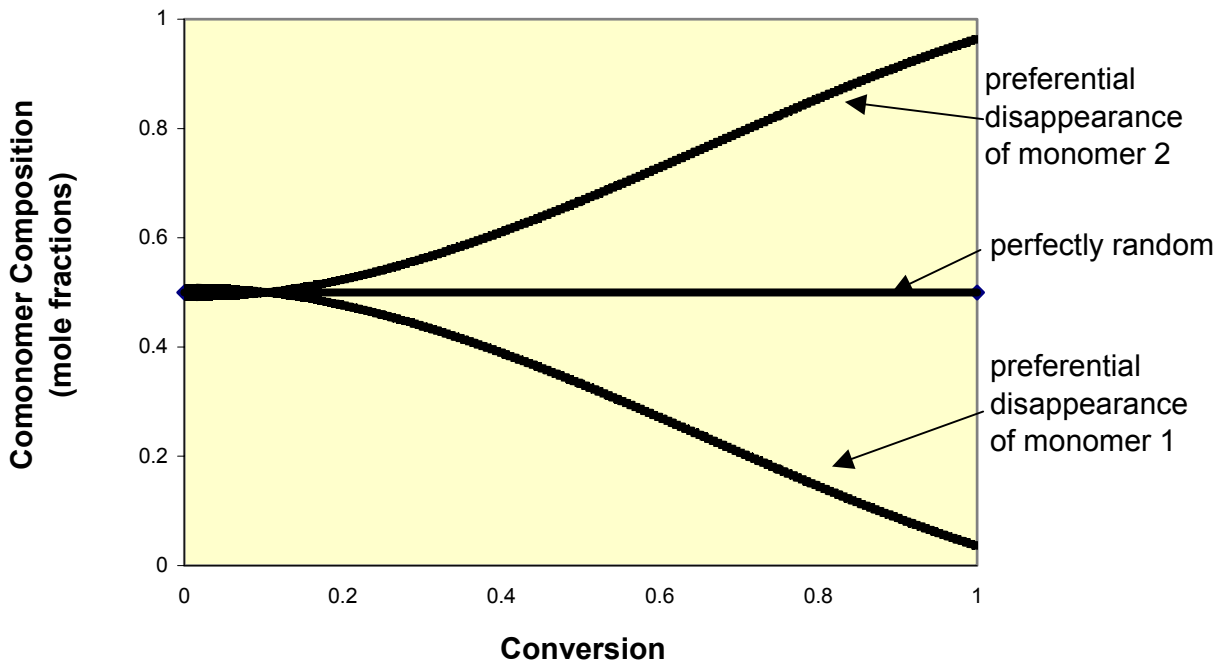


Figure 14: Hypothetical Comonomer Composition Change as a Function of Conversion

The disappearance of comonomer 1 is much faster than that of comonomer 2 as the figure shows. Therefore, near the end of the reaction, the copolymers that are produced will contain mostly comonomer 2 because comonomer 1 has already fully reacted. Clearly, the charge ratios that were introduced into the reaction vessel did not get incorporated into a short sequence copolymer in the same proportions.

AZEOTROPIC COPOLYMERIZATIONS

Copolymerizations that produce compositions with the same ratios of comonomers that were in the feed as that which was in the copolymer at, and only at, a narrow composition range are termed an azeotropic copolymerization.⁶² In other words, at the azeotropic composition, the exact amount of comonomer that is fed into the reaction will be uniformly incorporated into the copolymer. Therefore, perfectly statistical copolymers will be produced throughout the entire reaction. This type of copolymerization does not occur for every system, but can be used as a theoretical method of describing some copolymerizations. The term is derived from distillation behavior.⁶³

Figure 15 shows a plot of two theoretical copolymerizations where one is a perfectly statistical azeotropic copolymerization and the other is an example of a

perfectly random copolymerization. By plotting the copolymer compositions versus the starting feed compositions, one can determine the correct feed ratio of the comonomers to produce an azeotropic copolymerization. For this example in Figure 15, the feed ratio below 50 mole percent A produces a copolymer that contains a higher mole percent of monomer A incorporated into the copolymer than was introduced into the reaction. Above 50 mole percent of monomer A in the feed, a copolymer is produced that contains a lower mole percent monomer A than was fed into the reaction. Therefore, at 50 mole percent of each monomer fed into the system, theoretically, a copolymer will be produced that contains 50 mole percent of each comonomer.

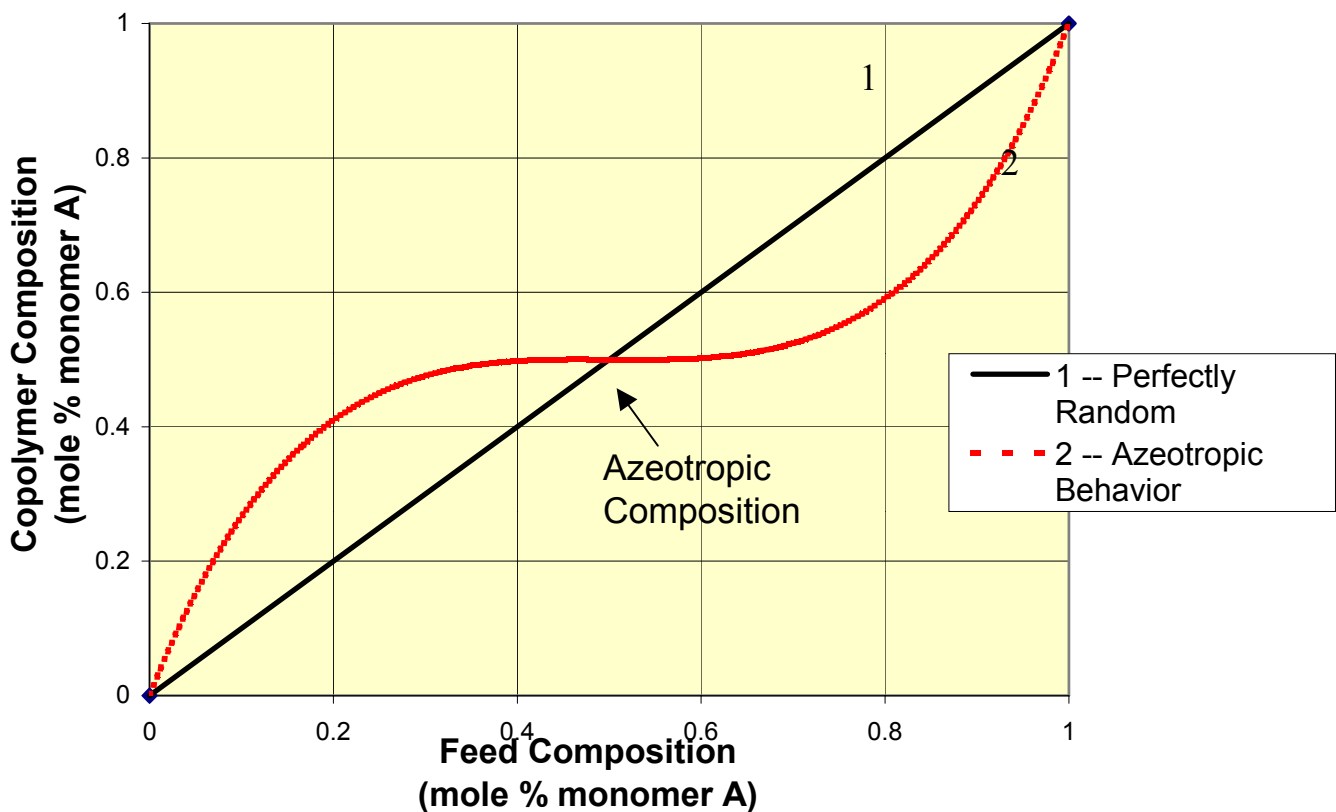


Figure 15: Illustrations of Perfectly Random vs. Azeotropic Copolymerization
(The former would show nearly identical reactivity ratios)

LITERATURE VALUES OF REACTIVITY RATIOS

Carbon fiber precursors are often made from acrylonitrile and methyl acrylate copolymers, which are typically produced in solution. Marvel and Schwen reported the reactivity ratios of acrylonitrile and methyl acrylate as 1.54 and 0.84, respectively,^{64,65} more than 40 years ago, but the methodology then did not allow for statistical confidence estimates. A more complete list of reactivity ratios is published in the Polymer Handbook and is the main source for such information.^{42,41} Marvel and Schwen determined the reactivity ratios of the system in 1957 when the analytical techniques were clearly not as advanced as they are today. Therefore, this study on acrylonitrile and methyl acrylate was designed to help clarify the copolymerization kinetics. Optimization of the copolymerization in order to produce a precursor of specific composition was one goal of this a study.

ISOLATED COPOLYMERS ANALYZED BY ¹H NMR

The copolymers that were isolated by precipitation and drying were subjected to ¹H NMR analysis to determine the copolymer composition. As described in the

experimental section, copolymer compositions were calculated from the integrated peaks for the methyl and methylene proton resonances, allowing the mole percent of AN in the copolymers to be obtained. The mole percents of MA incorporated into the copolymers were obtained by the difference.

The copolymer compositions were then plotted against the feed compositions for the seventeen different copolymerizations as shown in Figure 16. The straight line represents a perfectly random copolymerization and the curve represents the actual data for acrylonitrile. There is an inflection point at about 33 mole percent of acrylonitrile or 67 mole percent of methyl acrylate charged. The inflection point may be defined as the azeotropic composition for this system, where the feed ratio of 33/67 AN/MA mole percent is equivalent to the mole ratio in the copolymer.

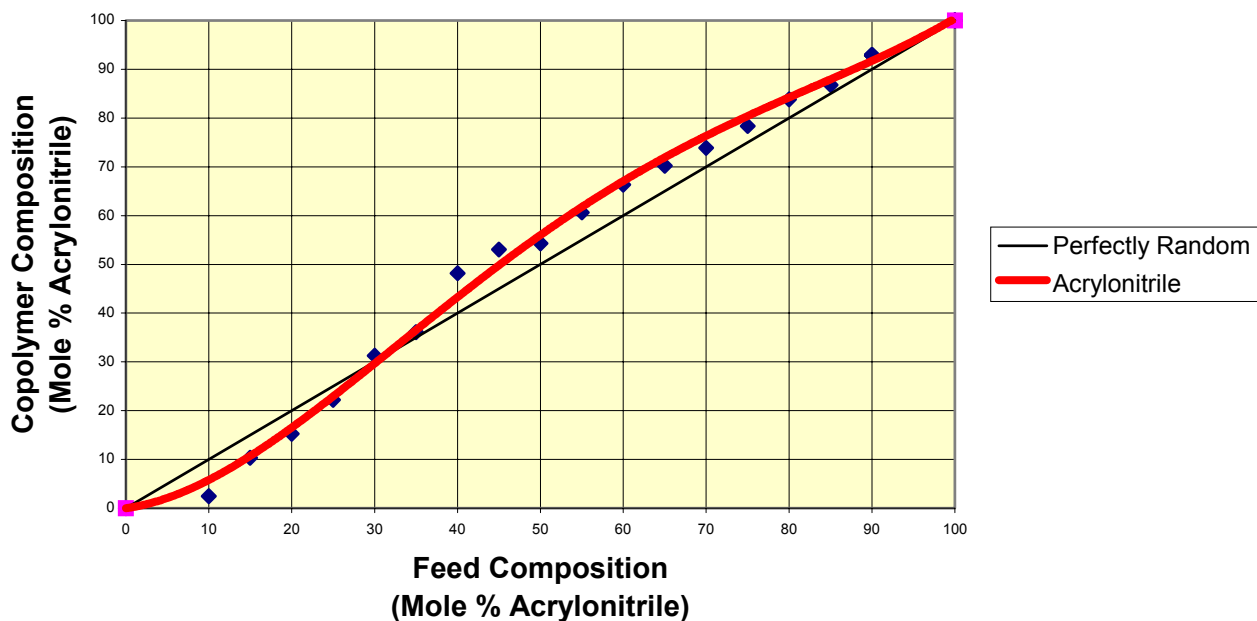


Figure 16: Feed Compositions versus Copolymer Compositions for Acrylonitrile

Compositions in Figure 16 needed for carbon fiber precursors should be above 85 mole percent of acrylonitrile. It would appear that at the feed compositions used for carbon fiber precursors, the amount of acrylonitrile being incorporated into the copolymer is higher than charged. However, the increased amount of acrylonitrile incorporation may be small enough that controlled copolymerizations produce approximately the correct amount of acrylonitrile in the copolymer.

REACTIVITY RATIO DETERMINATION

The seventeen different feed and copolymer composition data points were converted into molar fractions for use in the Mortimer/Tidwell nonlinear least squares method, using the computer program developed by van Herck.^{3,4} The computer program uses the mole fractions of the comonomer AN charged, the mole fraction of the comonomer incorporated into the copolymer, F_1 , and the value for the experimental F_1 minus the theoretical F_1 , which was denoted ΔF_1 . The theoretical value for F_1 was determined by using the differential form of the copolymer equation. This form is as follows:

$$F_1 = \frac{(r_1 f_1^2 + f_1 f_2)}{(r_1 f_1^2 + 2 f_1 f_2 + r_2 f_2^2)} \quad (59)$$

This equation gives the theoretical copolymer composition as the mole fraction of monomer M_1 in the copolymer, using literature values for reactivity ratios of 1.54 for AN and 0.84 for MA.^{64,65} Then the theoretical mole fraction was subtracted from the experimental mole fraction and the difference was the value for ΔF_1 . These calculations were performed for each set of data points. The differences in the theoretical and the experimental values ranged from 0.003 to -0.07 . These three sets of data, mole fraction of comonomer AN and mole fraction AN in copolymer and ΔF_1 , were programmed into the computer and calculations were conducted to determine the reactivity ratios. A 95% joint confidence limit was calculated along with the values for the reactivity ratios for the system. Figure 17 shows the results of the nonlinear least

squares calculations using the seventeen different feed and copolymer mole fractions. The single data point in the middle of the ellipse is the value for both reactivity ratios. The x-axis is the reactivity ratio for AN and the y-axis is the reactivity ratio for MA. The ellipse represents the 95% joint confidence limit where the reactivity ratios have a 95% statistical chance of having a value inside it.

The reactivity ratio for AN was determined to be 1.29 and the reactivity ratio for MA was determined to be 0.96. These values are a little different than the literature values, but are similar. The most important thing to note in Figure 17 is the 95% joint confidence limit. With this nonlinear least squares method of calculating the reactivity ratio, the possible error or 95% joint confidence limit was determined. As can be seen on the Figure 17 plot, the 95% joint confidence limit was obviously quite unattractively large.

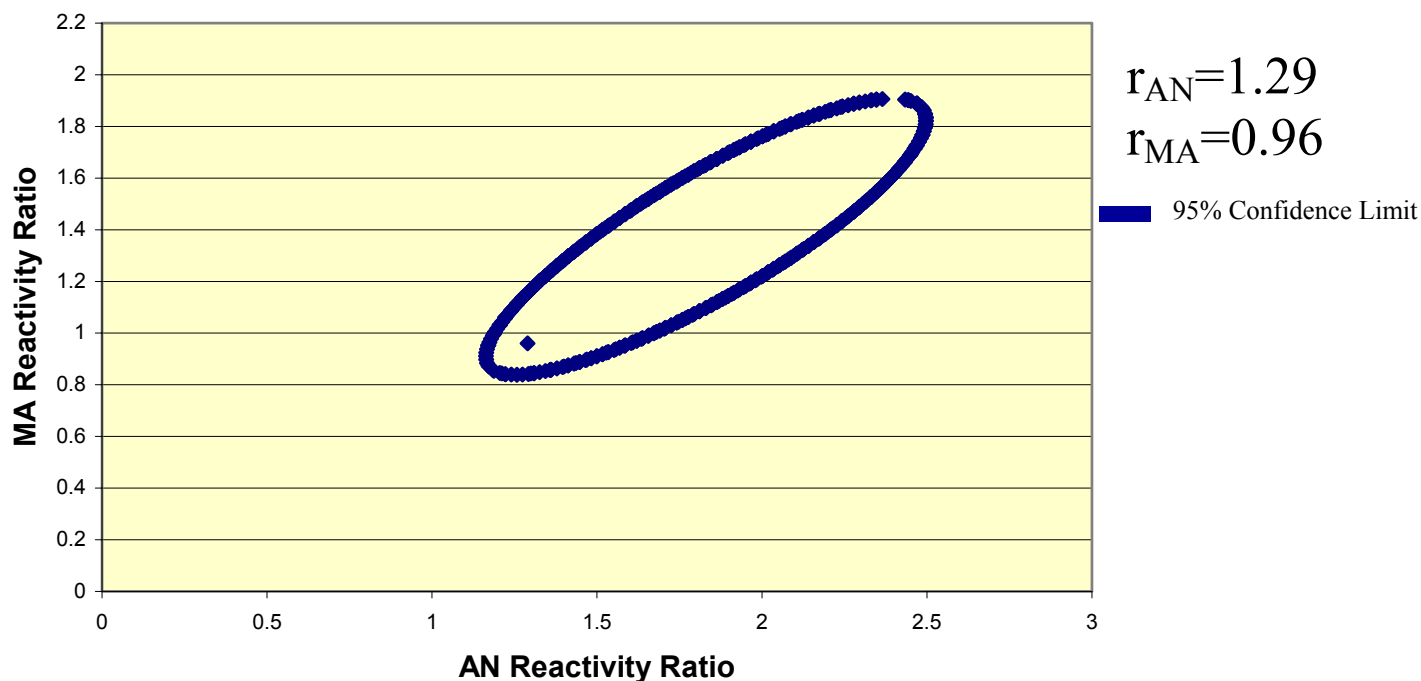


Figure 17: Mortimer/Tidwell Reactivity Ratio Plot with 95% Joint Confidence Limit
Based on Limited Data on Isolated Copolymers analyzed via Proton NMR

Therefore, in order to decrease the possible error that could occur in the experiments, more copolymers would need to be synthesized and studied. This would be time consuming and, therefore, an expensive study. Fortunately, the *in situ* real time FTIR experiments allowed for a much simpler approach than isolation and NMR analyses of the copolymers. The *in situ* FTIR method produced one data point every minute; therefore, as many as twenty five data points for the mole fractions can be determined in only one experiment. Isolating the copolymer and testing its composition by ^1H NMR yielded only one data point in each experiment.

REAL TIME *IN SITU* FTIR

The use of real time *in situ* FTIR as a tool for determining copolymer compositions is a relatively new development that yields a large amount of required differential copolymerization data from a few experiments.^{66,67} The disappearance of the comonomers was detected by the area under their FTIR signals. This permitted a direct quantitative measurement of the amount of comonomer that was being incorporated into the copolymer. The process of acquiring the copolymer composition data was rapid, precise and accurate.

The direct relationship between the disappearance of the monomer peaks and the production of the copolymers simplifies the calculations. The raw data that were produced from the *in situ* FTIR instrument were the decreasing peak areas under the two curves using the two-point base line as the lower corners of the triangular peaks. Measurements were taken every minute after the AIBN was added to the reaction flask and about twenty to thirty different data sets were obtained for each reaction. The set of data points for each reaction was thus similar to conducting the reaction twenty to thirty times and isolating the copolymer in order to determine the copolymer composition. The mole percent AN/MA feed ratios that were used in the *in situ* FTIR study were 90/10, 85/15, 80/20, 65/35, 50/50, 35/65 and 20/80. The copolymerization data were obtained at less than 9% conversion and, a total of 171 data points were obtained. One may emphasize that this is ten times the amount of isolated copolymer data that was obtained and analyzed by ¹H NMR.

The normalization of the peak areas that the *in situ* FTIR machine produced began by dividing each peak area by the initial peak area. Table 4 shows the conversion of the peak areas for the 85/15 mole percent reaction into normalized peak areas. The data shown are for only ten different scans made by the *in situ* FTIR instrument, but they also show the trend of the decreasing peak areas well.

Peak Areas			Normalized Peak Areas	
AN	MA		AN	MA
0.04973	0.06111		1	1
0.04879	0.06052		0.9811	0.9904
0.0483	0.05998		0.9713	0.9815
0.04777	0.0598		0.9605	0.9786
0.04755	0.05941		0.9561	0.9722
0.04695	0.05909		0.9442	0.9669
0.04682	0.05848		0.9415	0.957
0.04679	0.05819		0.941	0.9523
0.04667	0.05793		0.9385	0.9481
0.04621	0.05778		0.9294	0.9456

Table 4: *In situ* AN/MA FTIR copolymerization: Normalization of Peak Areas by Dividing the Peak Areas by the Initial Peak Area

After normalizing the peak areas by the initial peak area, the moles of the comonomers for each data set can be calculated. This set of data is an example of the 85/15 mole percent AN/MA reaction and the normalized data that was converted into moles of comonomers by multiplying by 0.85 for AN and 0.15 for MA. Table 5 shows the data conversion from the normalized peak areas for the ten decreasing peak areas to the moles of comonomers at each FTIR scan.

Normalized Peak Areas		Moles of Monomers	
AN	MA	AN	MA
1	1	0.85	0.15
0.9811	0.9904	0.834	0.1485
0.9713	0.9815	0.8256	0.1472
0.9605	0.9786	0.8165	0.1467
0.9561	0.9722	0.8127	0.1458
0.9442	0.9669	0.8026	0.145
0.9415	0.957	0.8003	0.1435
0.941	0.9523	0.7998	0.1428
0.9385	0.9481	0.7977	0.1422
0.9294	0.9456	0.7899	0.1418

Table 5: Conversion of Normalized Peak Areas to Moles of Monomer by Multiplying the Normalized Peak Areas by the 0.85 for AN and 0.15 for MA

The moles of the comonomers incorporated into the copolymer can then be calculated. The difference in the amount of moles from the initial values to the differential values for the moles of comonomers present at the time interval is directly equal to the number of moles that entered into the copolymer from time zero. Therefore, by calculating the difference between the initial data set and the differential data set gives the moles of comonomers that were incorporated into the copolymer at that certain scan. Table 6 shows the conversion of the moles of comonomers that were incorporated into the copolymer.

Moles of Comonomers			Moles in Copolymer	
AN	MA		AN	MA
0.85	0.15		0	0
0.834	0.1485		0.01598	0.001434
0.8256	0.1472		0.02434	0.00277
0.8165	0.1467		0.03349	0.003202
0.8127	0.1458		0.03726	0.004161
0.8026	0.145		0.04738	0.004953
0.8003	0.1435		0.04964	0.006444
0.7998	0.1428		0.05014	0.007154
0.7977	0.1422		0.05226	0.007784
0.7899	0.1418		0.06001	0.008156

Table 6: Conversion of the Moles of Comonomers to the Moles of Copolymers

The mole fraction of the comonomers can then be obtained. In order to get the mole fractions of the comonomers at the differential time interval of the peak area, the moles of each comonomer must be divided by the whole amount of the comonomers. So, for each set of data for the AN and MA moles of comonomers, the part is divided by the entire amount of moles at that time interval. Table 7 shows the conversion of the moles of comonomers of AN and MA at the different time intervals into the mole fractions of the comonomers. These data can then be used in the van Herck nonlinear least squares computer program to determine the reactivity ratios. However, the mole fractions of the comonomers incorporated into the copolymer must also be determined for the computer program.

Moles of Comonomers			Mole Fractions of	
			Comonomers	
AN	MA		AN	MA
0.85	0.15		0.85	0.15
0.834	0.1485		0.8488	0.1511
0.8256	0.1472		0.8486	0.1513
0.8165	0.1467		0.8476	0.1523
0.8127	0.1458		0.8478	0.1521
0.8026	0.145		0.8469	0.153
0.8003	0.1435		0.8479	0.152
0.7998	0.1428		0.8484	0.1515
0.7977	0.1422		0.8486	0.1513
0.7899	0.1418		0.8477	0.1522

Table 7: Conversion of Moles of Comonomers to Mole Fractions of Comonomers Present at the Differential Time Intervals

The mole fractions of the comonomers that were incorporated into the copolymer were then calculated from the moles of comonomers that were incorporated into the copolymer. The calculations were similar to those for the mole fractions of the comonomers. The moles of AN were divided by the sum of the moles at that differential time interval. Table 8 shows the conversion of the moles in copolymer to the mole fractions in the copolymer. These calculations use the part divided by whole in order to determine the mole fractions of the comonomers that were incorporated into the copolymer.

Moles in Copolymer		Mole Fractions in Copolymer	
AN	MA	AN	MA
0.01598	0.001434	0.9176	0.08237
0.02434	0.002771	0.9401	0.05995
0.03349	0.003202	0.9127	0.08725
0.03726	0.00416	0.8995	0.1004
0.04738	0.004953	0.9053	0.09463
0.04964	0.006443	0.8851	0.1148
0.05014	0.007154	0.8751	0.1248
0.05226	0.007784	0.8703	0.1296
0.06001	0.008156	0.8803	0.1196

Table 8: Conversion of the Moles in Copolymer of AN and MA into the Mole Fractions in the Copolymers

A plot of the mole fraction of the comonomer AN fed into the reaction versus the mole fraction of AN incorporated into the copolymer is shown in Figure 18. The straight line is an example of a perfectly random copolymerization or an azeotropic copolymerization and the curved line is the AN copolymerization curve. The curve indicates that below a feed ratio of about 0.38 mole fraction of AN, less AN was being incorporated into the copolymer than was charged. Above a value of 0.38 mole fraction of AN in the feed, more AN was incorporated into the copolymer. The opposite is obviously true for MA, where below 0.38 mole fraction MA in the feed, more is incorporated and above 0.38 mole fraction in the feed less is incorporated into the copolymer. Therefore, in order to predict the amount of each comonomer that will be in the product of this type of copolymerization, one can use Figure 18 as a reference.

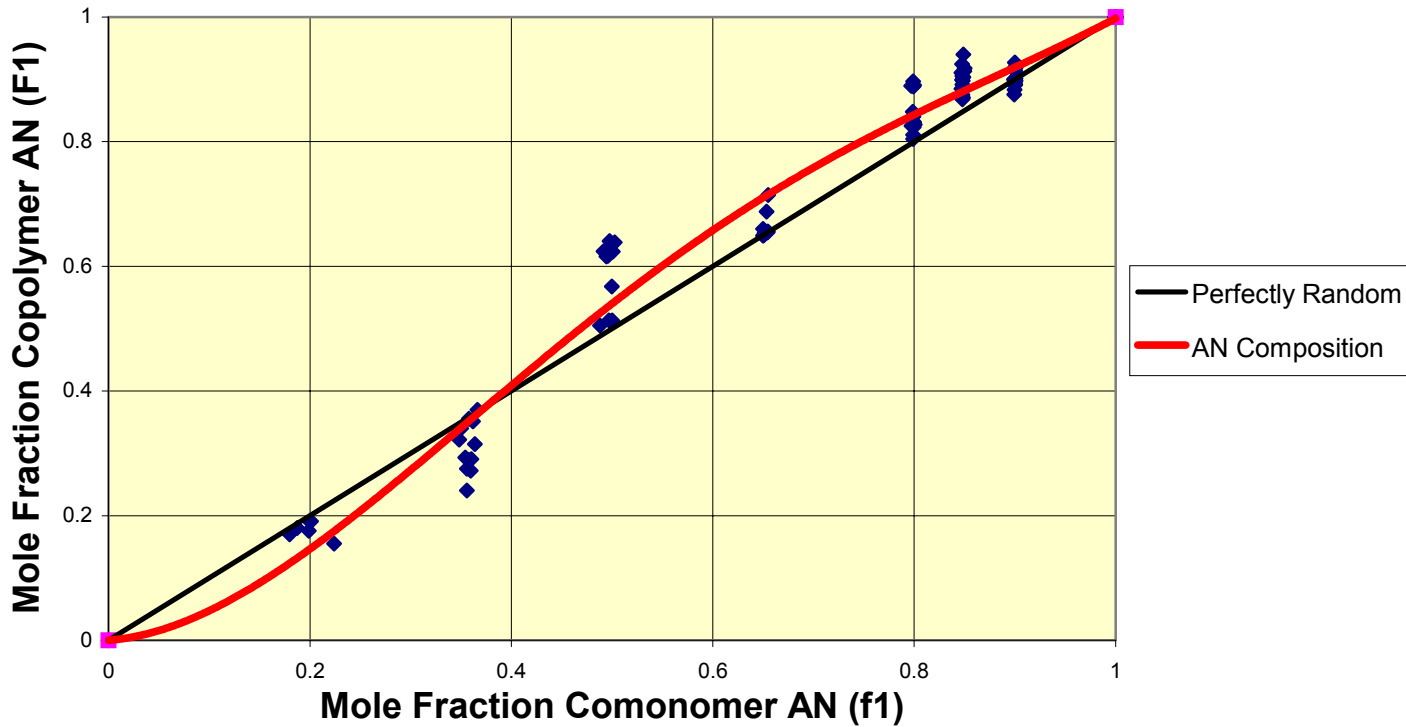


Figure 18: Copolymer Acrylonitrile Content Versus Acrylonitrile Content in the Feed

All of the 171 raw data points from the *in situ* FTIR instrument, eg. the mole fractions of the monomers fed into the reaction and the mole fractions of the monomers incorporated into the copolymer, were used in the calculations. As in the previous isolated copolymer calculations, the theoretical value for F_1 was calculated by starting with the literature values of 1.54 for AN and 0.84 for MA. The difference between the theoretical values and the experimental values were then calculated as described above to determine the value for ΔF_1 . Table 9 shows an example of the data that was calculated using the 85/15 mole percent AN/MA experiment.

Mole Fraction Comonomer AN	Mole Fraction Copolymer AN	Experimental F ₁ Minus Theoretical F ₁
f₁	F₁	delta F₁
0.85	0.9176	0.02321
0.8488	0.9401	0.04654
0.8486	0.9127	0.01934
0.8476	0.8995	0.00696
0.8478	0.9053	0.01257
0.8469	0.8851	-0.00697
0.8479	0.8751	-0.01768
0.8484	0.8703	-0.02288
0.8486	0.8803	-0.01307
0.8477	0.8928	9.58E-05

Table 9: Mole Fractions of AN in the Feed and in the Copolymer with values for delta F₁

The three values, mole fraction of comonomer AN in the feed and mole fraction of AN in the copolymer and delta F₁, were programmed into van Herck's computer program. Calculations were conducted on the data until the sum of the squares of the differences from the points to the curve were minimized. The reactivity ratios were determined by real time FTIR and the nonlinear least squares differential program to produce the plot in Figure 19. Reactivity ratios were again determined to be 1.29 for AN and 0.96 for MA. However, the 95% joint confidence limit shown by the ellipse

indicates that the uncertainty is much smaller than in the previous, more limited experiments.

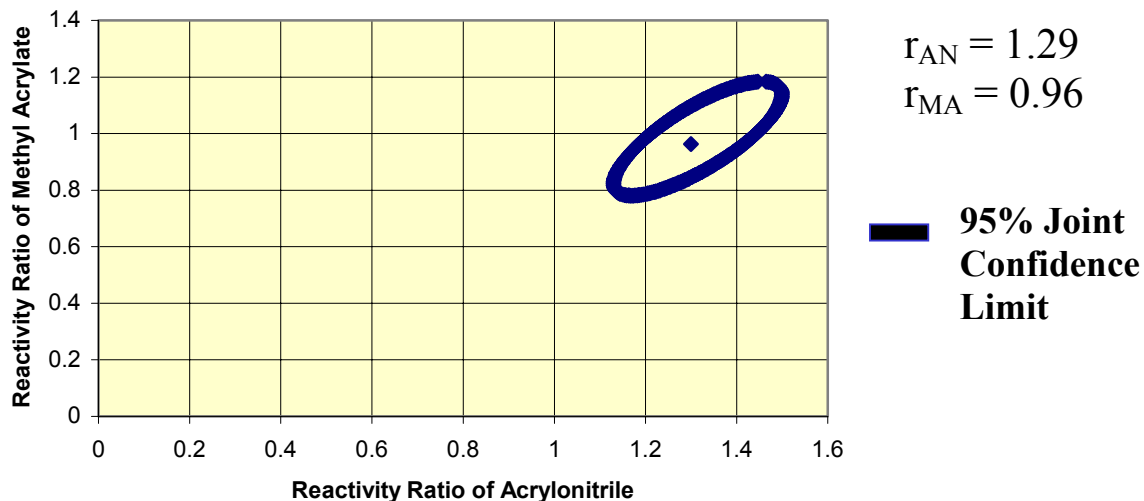


Figure 19: Reactivity Ratio Plot Using Real Time FTIR Data and Nonlinear Least Squared Differential Calculations

The ten-fold increase in data points decreased the possible uncertainty to ± 0.2 . Obviously, the more data points an experiment can obtain, the smaller the range of r_1 and r_2 that will lie within the 95% confidence ellipse. Therefore, the reactivity ratios obtained by the real time *in situ* FTIR instrument and the nonlinear least squares program determined more precise values for the reactivity ratios for AN and MA while being homogeneously polymerized in DMF and initiated with AIBN at 62°C.

Chapter V: Conclusions

Reactivity ratios for acrylonitrile and methyl acrylate have been reported in the literature, but accurate confidence limits and the quantitative validity of the values were not available. The Mortimer and Tidwell approach provides a nonlinear least squares method that can quantitatively determine the possible error that could be associated with the calculated reactivity ratios. Development of a computer program by van Herck that used the nonlinear least squares method of determining the reactivity ratios by the Mortimer and Tidwell approach, was critical to the development of the extensive calculations that were required.

This thesis determined that the azeotropic feed composition was about 37 mole percent AN and about 63 mole percent MA. The reactivity ratios for the AN/MA system were determined by using both ^1H NMR experiments on isolated copolymers and real

time *in situ* FTIR experiments. The ^1H NMR experiments required isolating and drying the copolymer in order to determine the amount of comonomer incorporated into the copolymer. This was a time consuming process and the results for the seventeen different copolymers that were produced were insufficient for precise determination of the reactivity ratios. The real time FTIR experiments produced ten times the data points in less time than the copolymerization and isolation of only three copolymers. Therefore, the extensive data helped determine more precise values for the reactivity ratios.

The calculations were conducted using nonlinear least squares equations and the 95% joint confidence limits were produced for each set of experiments. Both the ^1H NMR experiments and the *in situ* FTIR experiments determined the AN reactivity ratio to be 1.29 when conducted in DMF and initiated with AIBN at 62° C. The reactivity ratio for MA was determined to be 0.96 under similar conditions. The 95% confidence limit was calculated using the nonlinear least squares computer program. For the ^1H NMR experiments, the range of possible r_1 and r_2 values within the 95% confidence were large. However, the increased number of experimental data points that were obtained by the *in situ* FTIR instrument yielded smaller r_1 and r_2 ranges in the confidence limit. The values of the reactivity ratios within the 95% confidence limit were determined to be 1.29 +/- 0.2 for AN and 0.96 +/- 0.2 for MA.

The feed compositions needed for the carbon fiber precursors are considered to require greater than 85 mole percent AN. This study showed the incorporation of the AN monomer at these feed amounts to be modestly higher than that which was charged. The plots that were produced from the data in this thesis can be used to determine the amounts of monomers needed to produce a nearly uniform copolymer that would contain the

desired amount of AN and MA. Therefore, these results can also provide important information to relevant industrial processes of carbon fiber copolymer precursors.

Suggested Future Research:

The reactivity ratio study conducted in this thesis for PAN precursors for carbon fibers could be further refined by performing the same calculations using a non-linear least squares program to study terpolymers that contain for example, acrylonitrile, methyl acrylate and acryloxy benzophenone. Furthermore, determining if suspension polymerizations follow the same reaction kinetics as the solution polymerizations could give helpful insight into a more economically and environmentally friendly method of synthesizing AN/MA carbon fiber precursors. However, complications introduced in a suspension polymerization, such as different partition coefficients for the monomers and initiators between the aqueous and reacting phase, could prove to be a very challenging study.

Reactivity ratios could also be determined by using Real Time NMR to detect the disappearance of the monomers in DMSO-d₆ using AIBN as the initiator. The use of *in situ*-NMR to detect the disappearance of the monomers as the reaction proceeds could prove to be complimentary to the *in situ*-FTIR that was conducted in this study.

REFERENCES:

1. Tirrell, D. A. *Copolymerization*. In *Encyclopedia of Polymer Science and Engineering*; Mark, H. F.; Bikales, N. M.; Overberger, C. G.; Menges, G. Eds.; Wiley-Interscience: New York, 1986; Vol. 4; pp. 192-233.
2. Tidwell, P. W.; Mortimer, G. A. *J. Polym. Sci.: Part A* **1965**, *3*, 369.
3. van Herck, A. M. *J. Chem. Ed.* **1995**, *72*, 138.
4. van Herck, A. M.; Manders, B. G.; Smulders, W.; Aerdt, A. *Macromolecules* **1997**, *30*, 322-323.
5. Lee, S. M. *International Encyclopedia of Composites*; VCH: New York, 1990-91; Vol. 1.
6. Bacon, R.; Smith, W. H. *2nd Conf. Ind. Carbon and Graphite, Soc. Chim. Ind.* **1965**, *203*.
7. Shindo, A. *Report No. 317 Govt. Ind. Res. Instt. Osaka* **1961**.
8. Watt, W.; Phillips, L. N.; Johnson, W. *Engineer London* **1986**, *221*.
9. Bansal, R. C.; Donnet, J. B. *Carbon Fibers 2nd Ed.*; Marcel Dekker Inc.: New York, 1994.

10. Bhanu, V. A.; Wiles, K. B.; Banthia, A. K.; Mansuri, A.; Sankarpandian, M.; Rangarayan, P.; Glass, T. E.; Baird, D. G.; Wilkes, G. L.; McGrath, J. E. *Polymer Preprints* **2001**, *42*, 663.
11. Bhanu, V. A.; Wiles, K. B.; Rangarayan, P.; Baird, D. G.; McGrath, J. E. *SAMPE Proceedings* **2001**, *33*, 1499.
12. Bhanu, V. A.; Rangarayan, P.; Wiles, K. B.; Bortner, M.; Sankarpandian, M.; Godshall, D.; Glass, T. E.; Banthia, A. K.; Yang, J.; Wilkes, G. L.; Baird, D. G.; McGrath, J. E. *Polymer* **2002**, *43*, 2699-2709.
13. Rangarayan, P.; Yang, J.; Bhanu, V. A.; Godshall, D.; Wilkes, G. L.; McGrath, J. E.; Baird, D. G. *J. Appl. Polym. Sci.* **2002**, *85*, 69-83.
14. Wiles, K. B.; Bhanu, V. A.; Pasquale, A. J.; Long, T. E.; McGrath, J. E. *Polymer Preprints* **2001**, *41*, 608; *J. Polym. Sci.*, in press 2002.
15. Yang, J.; Banthia, A. K.; Godshall, D.; Rangarayan, P.; Wilkes, G. L.; Baird, D. G.; McGrath, J. E. *Polymer Preprints* **2000**, *41*, 59.
16. Donnet, J. B.; Bansal, R. C. *Carbon Fibers*; Marcel Dekker Inc.: New York, 1990.
17. Fitzer, E.; Frohs, W.; Heine, M. *Carbon* **1986**, *24*, 387.
18. Edie, D. *Carbon* **1998**, *36*, 345-362.
19. Sen, K.; Baharami, S. H.; Bajaj, P. In *High Performance Acrylic Fibers*, in J. M. S. *Revue of Macromolecular Chemistry Phys.*; Marcel Dekker Inc.: New York, 1996; Vol. C36; pp. 1-76.
20. Bajaj, P.; Padmanabhan, M. *Eur. Polym. J.* **1984**, *20*.
21. Bajaj, P. In *Manufactured Fibre Technology*; Gupta, V. B.; Kathari, V. K. Eds.; Chapman and Hall: London, 1997; pp. 407-454.
22. Bajaj, P. *Polymer* **2001**, *42*, 1707-1718.
23. O'Donnell, J. P.; Haddleton, D. M.; Morsley, D. R.; Richards, S. N. *J. Polym. Sci.* **1999**, *37*, 3549-3557.
24. Kim, B. K.; Oh, Y. S.; Lee, Y. M.; Yoon, L. K.; Lee, S. *Polymer* **2000**, *41*, 385-390.
25. Ebdon, J. R.; Huckerby, T. N.; Hunter, T. C. *Polymer* **1994**, *35*, 250-256.

26. Painter, P. C.; Coleman, M. M. *Fundamentals of Polymer Science*; Technomic Publishing Inc.: Lancaster, PA, 1997.
27. Odian, G. *Principles of Polymerization: 3rd Edition*; John Wiley and Sons Inc.: New York, 1991.
28. Moad, G.; Solomon, D. H. *The Chemistry of Free Radical Polymerization*; Pergamon Press: New York, 1995.
29. Rosen, S. L. *Fundamental Principles of Polymeric Materials*; John Wiley and Sons: New York, 1993.
30. Staudinger, H.; Schneiders, J. *Ann. Chim.* **1939**, *541*, 151.
31. Alfrey, T.; Bohrer, J. J.; Mark, H. *Copolymerization*; Interscience: New York, 1952.
32. Mayo, F. R.; Lewis, F. M. *J. Am. Chem. Soc.* **1944**, *66*, 1594.
33. Walling, C. *Free Radicals in Solution*; Wiley: New York, Chap. 4, 1957.
34. Flory, P. J. *Principles of Polymer Chemistry*; Cornell University Press: Ithaca, 1953.
35. Polic, A. L.; Duever, T. A.; Penlidis, A. *J. Polym. Sci.: Part A* **1998**, *36*, 813.
36. Davis, T. P. *J. Polym. Sci.: Part A* **2001**, *39*, 597.
37. Fineman, M.; Ross, S. D. *J. Polymer Sci.* **1950**, *5*, 259.
38. Kelen, T.; Tudos, F.; Turcsanyi, B. *Polymer Bull.* **1980**, *2*, 71-76.
39. Tudos, F.; Kelen, T.; Foldes-Bereznich, T.; Turcsanyi, B. *J. Macromol. Sci.: Part A* **1976**, *10*, 1513-1540.
40. Tudos, F.; Kelen, T. *J. Macromol. Sci.: Part A* **1981**, *16*, 1283.
41. Greenley, R. Z. In *Polymer Handbook 4th Edition*; Brandup, J.; Immergut, E. H.; Grulke, E. Eds.; John Wiley: New York, 1999.
42. Greenley, R. Z. In *Polymer Handbook Part II 3rd Ed.*; Brandup, J.; Immergut, E. H.; Grulke, E. Eds.; John Wiley: New York, 1989; pp. 153-265.
43. O'Driscoll, K. F.; Reilly, P. M. *Makromol. Chem., Makromol. Symp.* **1987**, *10/11*, 355.

44. O'Driscoll, K. F.; Kale, L. T.; Garcia-Rubio, L. H.; Reilly, P. M. *J. Polym. Sci.: Polym. Chem. Ed.* **1984**, *22*, 2777.
45. Hill, D. J. T.; O'Donnell, J. H. *Makromol. Chem., Makromol. Symp.* **1987**, *10/11*, 375.
46. Hill, D. J. T.; Lang, A. P.; O'Donnell, J. H.; O'Sullivan, P. W. *Eur. Polym. J.* **1989**, *25*, 911.
47. Hill, D. J. T.; Lang, A. P.; O'Donnell, J. H. *Eur. Polym. J.* **1991**, *27*, 765.
48. Hill, D. J. T.; Lang, A. P.; O'Donnell, J. H. *Eur. Polym. J.* **1991**, *27*, 765-772.
49. Mott, G.; Brendlein, W.; Braun, D. *Eur. Polym. J.* **1973**, *9*, 1007-1012.
50. Davis, T. P.; O'Driscoll, K. F.; Piton, M. C.; Winnik, M. A. *J. Polym. Sci.: Part C: Polym. Lett.* **1989**, *27*, 181.
51. Davis, T. P.; O'Driscoll, K. F.; Piton, M. C.; Winnik, M. A. *Macromolecules* **1990**, *23*, 2113.
52. Davis, T. P.; O'Driscoll, K. F.; Piton, M. C.; Winnik, M. A. *Polym. Int.* **1991**, *24*, 65.
53. Ghi, P. Y.; Hill, D. J. T.; O'Donnell, J. H.; Pomeroy, P. J.; Whittaker, A. K. *Polymer Gels and Networks* **1996**, *4*, 253.
54. Hagiopol, C. *Copolymerization: Toward a Systematic Approach*; Kluwer Academic: New York, 1999.
55. Biesenberger, J. A.; Sebastian, D. H. *Principles of Polymerization Engineering*; Wiley: New York, 1983.
56. Brandolini, A. J. *NMR Spectra of Polymer and Polymer Additives*; Marcel Dekker: New York, 2000.
57. Tonelli, A. E. *NMR Spectroscopy and Polymer Microstructures: The Conformational Connection*; VCH: New York, 1989.
58. Macomber, R. S. *NMR Spectroscopy: Essential Theory and Practice*; Brace Jovanovich Publishers: New York, 1988.
59. Wu, C. *Handbook of Size Exclusion Chromatography*; Dekker: New York, 1995.
60. Buback, M.; Tups, H. *Makromol. Chem. Rapid Commun.* **1987**, *8*, 123.

61. Storey, R. F.; Donnalley, A. B.; Maggio, T. L. *Macromolecules* **1998**, *31*, 1523.
62. Alfrey, T.; Howard, H. C.; Lewis, C. W. *J. Am. Chem. Soc.* **1952**, *74*, 4856-4858.
63. Fritzweiler, R.; Dietrich, K. R. *International Sugar Journal* **1933**, *35*, 29-32, 71-74.
64. Marvel, C. S.; Schwen, R. *J. Am. Chem. Soc.* **1957**, *79*, 6003.
65. Okamura, S.; Yamashita, T. *J. Soc. Textile and Cellulose Ind. Japan*, **1953**, *9*, 444.
66. Pasquale, A. J.; Long, T. E. *Macromolecules* **1999**, *32*, 7954-7957.
67. Pasquale, A. J., Ph.D. Dissertation, Chemistry, Virginia Polytechnic Institute and State University 2002.

Vita:

Kenton Broyhill Wiles, son of Mr. and Mrs. A. D. Wiles II, was born on July 22, 1975 in Indianapolis, Indiana. He was raised in Noblesville, IN, and graduated from Orchard Country Day School Elementary and Junior High located in Indianapolis. In 1994, Kent graduated from Noblesville High School. He then moved to Bloomington, IN in the spring of 1995 and began his career in science at Indiana University as an undergraduate. After graduation in December of 1998, Kent accepted employment as a synthetic polymer chemist at Reilly Industries in Indianapolis. After a summer as a bench chemist, Kent entered the polymer chemistry graduate program at Virginia Polytechnic Institute and State University under the guidance of Professor James E. McGrath, during which time he presented papers at two national conferences of the American Chemical Society. He obtained his Masters in Chemistry in 2002. His immediate plans include further study at Virginia Tech as a Doctor of Philosophy candidate in Macromolecular Science and Engineering.